# NEU1 Sialidase Expressed in Human Airway Epithelia Regulates Epidermal Growth Factor Receptor (EGFR) and MUC1 Protein Signaling*[S]

Erik P. Lillehoj[‡§], Sang Won Hyun[§], Chiguang Feng[¶], Lei Zhang[¶], Anguo Liu[§], Wei Guang[‡], Chinh Nguyen[§], Irina G. Luzina[∥], Sergei P. Atamas[∥], Antonino Passaniti**, William S. Twaddell**, Adam C. Puché[‡‡], Lai-Xi Wang[§§¶¶], Alan S. Cross[¶∥], and Simeon E. Goldblum[§∥**1]

From the Departments of ‡Pediatrics, ∥Medicine, **Pathology, ‡‡Anatomy and Neurobiology, and ¶¶Biochemistry and Molecular Biology, §Mucosal Biology Research Center, ¶Center for Vaccine Development, and §§Institute of Human Virology, University of Maryland School of Medicine, Baltimore, Maryland 21201

**Background:** Airway epithelia express sialoglycoproteins that respond to danger signals and initiate repair programs.
**Results:** NEU1 sialidase desialylates EGFR and MUC1 in airway epithelia to regulate their responsiveness to ligands and adhesiveness to *P. aeruginosa*.
**Conclusion:** NEU1 provides an additional level of regulation over airway epithelial responsiveness to ligands and pathogens.
**Significance:** The downstream effects of EGFR desialylation require further investigation.

Epithelial cells (ECs) lining the airways provide a protective barrier between the external environment and the internal host milieu. These same airway epithelia express receptors that respond to danger signals and initiate repair programs. Because the sialylation state of a receptor can influence its function and is dictated in part by sialidase activity, we asked whether airway epithelia express catalytically active sialidase(s). Human primary small airway and A549 ECs expressed NEU1 sialidase at the mRNA and protein levels, and NEU1 accounted for >70% of EC sialidase activity. Blotting with *Maackia amurensis* and peanut agglutinin lectins established epidermal growth factor receptor (EGFR) and MUC1 as *in vivo* substrates for NEU1. NEU1 associated with EGFR and MUC1, and NEU1-EGFR association was regulated by EGF stimulation. NEU1 overexpression diminished EGF-stimulated EGFR Tyr-1068 autophosphorylation by up to 44% but enhanced MUC1-dependent *Pseudomonas aeruginosa* adhesion by 1.6–1.7-fold and flagellin-stimulated ERK1/2 activation by 1.7–1.9-fold. In contrast, NEU1 depletion increased EGFR activation (1.5-fold) and diminished MUC1-mediated bacterial adhesion (38–56%) and signaling (73%). These data indicate for the first time that human airway epithelia express catalytically active NEU1 sialidase that regulates EGFR- and MUC1-dependent signaling and bacterial adhesion. NEU1 catalytic activity may offer an additional level of regulation over the airway epithelial response to ligands, pathogens, and injurious stimuli.

Epithelial cells (ECs)[2] lining the airways provide a protective barrier between the external environment and the internal host milieu (1). The EC surface is armed with numerous receptors and adhesion molecules that recognize and respond to host mediators, inflammatory cells, and exogenous danger signals. A complex veneer of highly sialylated structures contribute to the airway epithelial barrier. In eukaryotic cells, glycoproteins and glycolipids expressed on the surface contain oligosaccharide chains whose outermost positions are terminated with *N*-acetylneuraminic acid (2, 3). The sialic acid (SA) family of >50 closely related but structurally diverse nine-carbon monosaccharides with their terminal location and negative charge are strategically positioned to influence intermolecular and cell-cell interactions through steric hindrance and/or electrostatic repulsion. These highly electronegative, hydrophilic residues influence protein tertiary conformation and bioactivity and can protect them against proteolysis. The human respiratory EC surface is decorated with both α-2,3-linked and α-2,6-linked SAs (4). Superimposed on this highly sialylated surface are specific receptors that are themselves sialylated. Finally, the airway EC surface and all of its receptors are overlaid with a constantly moving, SA-rich, mucous blanket (5).

In response to disruptive, denuding injury, the epithelium utilizes an epidermal growth factor receptor (EGFR)-driven repair program centering around phospholipase Cγ-mediated cell migration (1). EGFR is itself sialylated (6), and gangliosides, sialylated glycosphingolipids present in the outer leaflet of all plasma membranes, regulate ligand-dependent and ligand-independent EGFR autophosphorylation (7, 8). Similarly, mucin-1 (MUC1) is a heavily sialylated membrane-bound gly-

2 The abbreviations used are: EC, epithelial cell; Ad, adenovirus; EGFR, epidermal growth factor receptor; MAL, *M. amurensis* lectin II; m.o.i., multiplicity of infection; MUC1, mucin-1; NANA, *N*-acetylneuraminic acid; 4-MU-NANA, 2′-(4-methylumbelliferyl)-α-D-*N*-acetylneuraminic acid; NEU, neuraminidase; PNA, peanut agglutinin; qRT-PCR, quantitative RT-PCR; SA, sialic acid; SAEC, small airway EC; TLR, Toll-like receptor; GM3, sialosyllactosylceramide; GM1, monosialotetrahexosylganglioside; SH2, Src homology 2.

coprotein that influences a diverse range of functions, including cell-cell and cell-matrix adhesion, cell motility, and host cell-pathogen interactions (9). On the cell surface, MUC1 interacts with EGFR and modifies EGFR-driven signaling (10). Together with the pattern recognition receptor Toll-like receptor (TLR) 5, MUC1 binds to bacterial flagellin, and both receptor-ligand interactions are coupled to downstream signaling (10–12). In addition to MUC1, airway epithelia also express other sialylated surface molecules that serve as recognition motifs for pathogenic viruses and bacteria and their toxins (13). In fact, a conserved virulence factor for many respiratory pathogens is the expression of neuraminidase (14).

The sialylation state of glycoconjugates is dynamically and coordinately regulated through the opposing catalytic activities of sialyltransferases and sialidases (15, 16). Sialidases hydrolyze the glycosidic linkage between SAs and the subterminal sugar of glycoconjugates. Four mammalian sialidase/neuraminidases (NEUs) have been identified, NEU1, -2, -3, and -4 (17–21). NEU1 is localized to lysosomes and is only active in association with cathepsin A and $\beta$-galactosidase. NEU2 is found in the cytosol, NEU3 is associated with the plasma membrane, and NEU4 is located in mitochondria. As members of the neuraminidase/sialidase superfamily, each contains one or more of the conserved so-called Asp boxes, an amino acid sequence comprising -$SXDXGXTW$- where $X$ represents variable residues, together with the -(F/Y)RIP- motif (16). Although the expression and function of mammalian sialidases have been documented in selected tissues and species, whether human respiratory epithelia express one or more sialidases is unknown. In these studies, we have established that human airway ECs express sialidase catalytic activity, much of which can be ascribed to NEU1. Furthermore, we have established two important receptors expressed in airway epithelia, EGFR and MUC1, as *in vivo* substrates for NEU1 and that NEU1 regulates the responsiveness of these two receptors to their respective ligands as well as epithelial adhesiveness to bacteria.

## EXPERIMENTAL PROCEDURES

*Reagents*—Unless otherwise stated, all chemical reagents were from Sigma. 2-Deoxy-NANA was from Calbiochem. *N*-Acetylneuraminic acid was from Research Products International (Mt. Prospect, IL). NEU1-, NEU3-, and MUC1-targeting small interfering (si) RNAs and their respective non-targeting control siRNAs were from Dharmacon (Lafayette, CO). Lipofectamine and protein G-agarose were from Invitrogen. Oligonucleotide primers for quantitative (q) RT-PCR were synthesized at the University of Maryland Biopolymer and Genomics Core Facility (Baltimore, MD). Reagents for qRT-PCR were from Qiagen (Valencia, CA), Promega (Madison, WI), and Invitrogen. Precast sodium dodecyl sulfate (SDS)-polyacrylamide gels were from Novex (San Diego, CA). Polyvinylidene fluoride (PVDF) membrane was from Millipore (Bedford, MA). Enhanced chemiluminescence reagents and prestained protein molecular weight markers were from Amersham Biosciences. Rabbit anti-human NEU1 antibody was from Rockland Immunochemicals (Gilbertsville, PA). Mouse anti-human EGFR, mouse anti-human phospho-EGFR (Tyr-1068), mouse anti-human phospho-ERK1/2, and mouse anti-human ERK2 primary

antibodies and horseradish peroxidase (HRP)-conjugated goat anti-rabbit and goat-anti-mouse secondary antibodies were from BD Biosciences. Mouse anti-cathepsin A, anti-LAMP1, and anti-TLR5 antibodies were from Santa Cruz Biotechnology (Santa Cruz, CA). Rabbit anti-human EGFR was from Thermo Scientific (Rockford, IL). Mouse anti-human MUC1 antibody was from Biomeda (Foster City, CA). Mouse anti-*Physarum* $\beta$-tubulin antibody was from Roche Applied Science. Mouse anti-FLAG and rabbit anti-hemagglutinin (HA) antibodies were from Cell Signaling Technology (Danvers, MA). Cy3-conjugated goat anti-rabbit secondary antibody was from Jackson ImmunoResearch Laboratories (West Grove, PA). Biotinylated goat anti-rabbit secondary antibody was from Dako (Carpinteria, CA). Recombinant human EGF was from R&D Systems (Minneapolis, MN). Biotinylated *Maackia amurensis* lectin II (MAL) and biotinylated *Arachis hypogaea* (peanut agglutinin (PNA)) were from Vector Laboratories (Burlingame, CA). Protein assay dye reagent and Macro-Prep High S and Macro-Prep High Q supports were from Bio-Rad. Polymyxin B-agarose was from Pierce.

*Human Airway EC Cultures*—Human respiratory ECs derived from distinct regions of the airway, including the trachea (1HAEo⁻ and CFTE29o⁻ cells), bronchus (16HBE14o⁻ and BEAS-2B cells), terminal bronchioles (small airway ECs (SAECs)), and alveolus (A549 cells), were studied. A549 cells are an alveolar type II cell line derived from a lung adenocarcinoma (American Type Culture Collection, Manassas, VA). 16HBE14o⁻, CFTE29o⁻, and 1HAEo⁻ are SV40 T antigen-transformed cell lines that were provided by Dr. Dieter Gruenert (California Pacific Medical Center Research Institute, San Francisco, CA). BEAS-2B is an SV40-transformed cell line that was provided by Dr. Sekhar Reddy (The Johns Hopkins University, Baltimore, MD). Cells were cultured in Dulbecco's modified Eagle's medium (DMEM) containing 10% fetal bovine serum (Hyclone Laboratories, Logan, UT), 50 units/ml penicillin, and 50 $\mu$g/ml streptomycin. Human primary SAECs (Lonza, Walkersville, MD) were cultured in predefined small airway growth medium (Lonza) containing hydrocortisone, human EGF, epinephrine, transferrin, insulin, retinoic acid, triiodothyronine, and fatty acid-free bovine serum albumin as described (22). Only SAEC passages 2–4 were studied.

*Fluorometric Assay for Sialidase Activity*—SAECs and A549 cells ($1.0 \times 10^6$ cells/reaction) were suspended in 200 $\mu$l of 500 mM sodium acetate, pH 4.4 containing 0.1% Triton X-100 and protease inhibitor mixture (Roche Applied Science) and then incubated for 1 h at 37 °C with 25 $\mu$l of 2.0 mM 2'-(4-methylumbelliferyl)-$\alpha$-D-N-acetylneuraminic acid (4-MU-NANA), mixing the tubes every 15 min. The sialidase reaction was terminated by addition of 133 mM glycine, pH 10.3, 60 mM NaCl, and 0.083 M $Na_2CO_3$ after which the fluorescence intensity was measured with a Bio-Rad fluorometer (excitation at 355 nm; emission at 460 nm). In selected experiments, EC preparations were boiled (100 °C for 10 min) prior to the assay. In other experiments, ECs were preincubated with either the competitive neuraminidase inhibitor 2-deoxy-NANA (5.0–500 $\mu$g/ml) (23) or purified *N*-acetylneuraminic acid (1.0–50 mM). A molecule with comparable molecular weight and charge to 2-de-

**TABLE 1**

Oligonucleotide primers used for quantitative RT-PCR

F, forward primer; R, reverse primer; HPRT, hypoxanthine-guanine phosphoribosyltransferase.

| RNA target | Primer sequence | PCR product size | GenBank accession no. |
|---|---|---|---|
| | | *bp* | |
| NEU1 | F, 5′–TGTGACCTTCGACCCTGAGC–3′ | 124 | NM_000434 |
| | R, 5′–TCGCAGGGTCAGGTTCACTC–3′ | | |
| NEU2 | F, 5′–AGTGGTCCACCTTTGCAGTG–3′ | 143 | NM_005383 |
| | R, 5′–ATGGCTGAGGAAGCAGAAGG–3′ | | |
| NEU3 | F, 5′–AATGTGAAGTGGCAGAGGTGA–3′ | 148 | NM_006656 |
| | R, 5′–TCACAGAGCTGTCGACTCAGG–3′ | | |
| NEU4 | F, 5′–TGCTGGTACCCGCCTACAC–3′ | 103 | NM_080741 |
| | R, 5′–CCGTGGTCATCGCTGTAGAA–3′ | | |
| HPRT | F, 5′–ACCAGTCAACAGGGGACATAAAAG–3′ | 102 | NM_000194 |
| | R, 5′–GTCTGCATTGTTTGCCAGTGTC–3′ | | |

oxy-NANA, 2-keto-3-deoxyoctulosonic acid, was used as a negative control (24).

*Sialidase Activity for Ganglioside Substrate*—SAECs and A549 cells were suspended in 200 $\mu$l of 50 mM sodium acetate, pH 4.4 containing 0.1% Triton X-100 and protease inhibitor mixture. The cell suspensions were mixed with 25 $\mu$l of a bovine brain ganglioside mixture (2.0 mg/ml; Calbiochem) and incubated for 1 h at 37 °C. The reaction was terminated by addition of 25 $\mu$l of 1.33 M glycine, pH 10.3, 0.6 M NaCl, and 0.42 M Na$_2$CO$_3$. Released SA was quantified by high pH anion-exchange chromatography with pulsed amperometric detection as described (23). For each assay, serial dilutions of known concentrations of pure *N*-acetylneuraminic acid were measured, and a standard curve was generated. The SA concentration in each sample was interpolated from the standard curve using GraphPad Prism 4 (GraphPad Software, La Jolla, CA). The background concentration of SA spontaneously released from the simultaneous cell-free ganglioside control was subtracted from each value.

*qRT-PCR for NEU1, -2, -3, and -4*—Total cellular RNA was extracted from SAECs using TRIzol reagent (Invitrogen). RNA purity was established with the 260/280 nm absorption ratio (>1.90). Total RNA (1.0 $\mu$g) was treated with DNase I (Invitrogen) for 15 min and reverse transcribed using avian myeloblastosis virus reverse transcriptase and poly(T) primer (Promega). The resulting cDNA was quantified by PCR using SYBR Green PCR Master Mix and an ABI Prism 7900HT cycler. Primers for detection of NEU1, NEU2, NEU3, NEU4, and hypoxanthine-guanine phosphoribosyltransferase mRNAs were designed using Primer Express 2.0 and are indicated in Table 1. The levels of NEU1, NEU2, NEU3, and NEU4 transcripts were normalized to hypoxanthine-guanine phosphoribosyltransferase transcripts using the $2^{-\Delta\Delta Ct}$ method (25).

*Immunoblotting for NEU1, Cathepsin A, and MUC1*—Cells were thoroughly rinsed with ice-cold HEPES buffer and lysed with ice-cold 50 mM Tris-HCl, pH 8.0, 1.0% Nonidet P-40, 0.5% SDS, 150 mM NaCl, 0.1 mM phenylmethylsulfonyl fluoride, 5.0 $\mu$g/ml leupeptin, 1.0 mg/ml pepstatin A, 1.0 mg/ml aprotinin, 1.0 mM vanadate, 1.0 mM sodium fluoride, 10 mM disodium pyrophosphate, 500 $\mu$M *p*-nitrophenol, and 1.0 mM phenylarsine oxide as described (26). The cell lysates were assayed for protein concentration with the Bio-Rad Protein Assay Dye Reagent. Equal amounts of protein were resolved by electrophoresis on 8–16% SDS-polyacrylamide gels and transferred to PVDF membranes. In some experiments, the blots were

blocked for 1 h using 5.0% nonfat milk in 50 mM Tris-HCl, pH 8.0, 150 mM NaCl, and 0.01% Tween 20 (TBS-T); probed with either rabbit anti-human NEU1 antibody or murine anti-human cathepsin A antibody, each followed by HRP-conjugated goat anti-rabbit antibody and horse anti-mouse antibody, respectively; and developed with enhanced chemiluminescence (ECL) reagents (26). In other experiments, blots were probed with mouse anti-human MUC1 antibody followed by HRP-conjugated goat anti-mouse antibody. To confirm equivalent protein loading and transfer, blots were stripped with 62.5 mM Tris-HCl, pH 6.7, 100 mM 2-mercaptoethanol, and 2.0% SDS; washed with TBS-T; reprobed with mouse anti-*Physarum* $\beta$-tubulin antibody followed by HRP-conjugated goat anti-mouse antibody; and developed with ECL reagents.

*Adenoviral Constructs Encoding FLAG-tagged NEU1 and HA-tagged NEU3*—To regulate NEU1 and NEU3 expression in SAECs and A549 cells, recombinant adenovirus (Ad) encoding FLAG-tagged human NEU1 (Ad-NEU1) and HA-tagged human NEU3 (Ad-NEU3) were generated as described for Ad encoding other gene products (22). The full-length human NEU1 (GenBank$^{TM}$ accession number NM_000434.3) and NEU3 (GenBank accession number NM_006656.5) sequences were synthesized by Primm Biotech (Cambridge, MA) after which the 3× FLAG tag and HA tag sequences were inserted prior to the stop codon at the 3′-end of the NEU1 and NEU3 sequences, respectively. The recombinant Ad-NEU1 and Ad-NEU3 were generated using the AdEasy Adenoviral Vector System (Stratagene, La Jolla, CA) according to the manufacturer's recommendation. Briefly, each was subcloned into the pShuttle-IREs-hrGFP-1 shuttle vector using restriction enzyme digestion and ligation. Each resultant shuttle plasmid was linearized by PmeI digestion and, with the Ad backbone plasmid (pAdEasy-1, Qbiogene/MP Biomedicals, Solon, OH), was used to co-transform electrocompetent *E. coli* BJ5183 cells to produce recombinant plasmids. As a negative control, an Ad-Null plasmid was generated using pAdEasy-1 and pShuttle-IREs-hrGFP-1 in the absence of an insert. Recombinant plasmids were selected for kanamycin resistance and screened for recombination by PacI digestion. Recombinant plasmids were used to transform XL10-Gold cells, and bacterial lysates were passed through Maxiprep columns (Qiagen) for plasmid purification. Ad-NEU1 and Ad-NEU3 each were linearized with PacI digestion and transfected in the presence of Lipofectamine into AD-293 cells. After 7–10 days, cells were scraped off flasks with a rubber policeman and subjected to three freeze-thaw

cycles, and virus was harvested in the supernatants for presentation to fresh AD-293 cells and titration in a plaque-forming assay. SAECs and A549 cells were transiently infected with packaged Ad-NEU1 or Ad-NEU3 at increasing multiplicities of infection and after 24 h were lysed, and the lysates were processed for FLAG or HA immunoblotting.

*Knockdown of NEU1, NEU3, and MUC1 through siRNA Technology*—SAECs and A549 cells were transfected with siRNA duplexes designed to specifically target NEU1, NEU3, or MUC1 or irrelevant control siRNA duplexes not corresponding to any known sequence in the human genome as described (27). For transfection, $5.0 \times 10^5$ ECs were centrifuged ($200 \times g$ for 10 min), and the cell pellet was resuspended in 100 $\mu$l of Amaxa Nucleofactor solution (Lonza) with 2.7 $\mu$g of siRNA duplexes. The EC-siRNA mixture was transferred to an Amaxa-certified cuvette and subjected to programmed electroporation (program X-001). The transfected cells were cultured for 24–72 h after which they were lysed, and the lysates were processed for NEU1 and MUC1 immunoblotting. In other experiments, A549 cells were transiently infected with packaged Ad-NEU1 or Ad-Null vector control, each at a multiplicity of infection (m.o.i.) of 100. After 48 h, NEU1-targeting or control siRNAs were introduced into A549 cells overexpressing FLAG-tagged NEU1. To exclude off-target effects, A549 cells overexpressing HA-tagged NEU3 were transfected with NEU1-targeting, NEU3-targeting, or control siRNAs. After 24–72 h, the transfected cells were lysed and processed for immunoblotting with mouse anti-FLAG or rabbit anti-HA antibody. To confirm equivalent protein loading, blots were stripped and reprobed for $\beta$-tubulin. These siRNA-transfected epithelia were studied for sialidase activity, lectin blotting, EGFR or ERK1/2 activation, and bacterial adhesion.

*Immunolocalization of NEU1 in A549 Cells*—A549 cells were cultured overnight in 8-well glass chamber slides (Nunc/Thermo Fisher, Waltham, MA). The cells were washed three times with PBS, fixed with 4% paraformaldehyde in PBS for 10 min at 22 °C, washed, permeabilized with 0.5% Triton X-100 in HEPES buffer for 10 min at 4 °C, blocked with 1% donkey serum for 30 min, and incubated overnight at 4 °C with anti-NEU1 antibody (1:500 dilution in 1.0% donkey serum). The slides were washed and incubated with Cy3-conjugated goat anti-rabbit secondary antibody. DAPI was used to counterstain nuclei. After mounting with Vectashield (Vector Laboratories), the immunostained ECs were analyzed and photographed using an Olympus FluoView 500 laser-scanning confocal fluorescence microscope fitted with a 60×, numerical aperture 1.4 objective and standard excitation/emission filters for detection of DAPI and Cy3. Images were cropped and assembled into panels with Adobe Photoshop 4.0.

*Detection of NEU1 in Lysosomes*—A549 cells were processed for isolation of lysosomes using the Lysosome Isolation kit (Sigma) following the manufacturer's protocol. Lysosomal proteins were resolved on 8–16% SDS-polyacrylamide gels, transferred to PVDF membranes, and processed for immunoblotting with anti-NEU1 and anti-LAMP1 antibodies.

*NEU1-EGFR and NEU1-MUC1 Co-immunoprecipitation Assays*—A549 cells were infected with increasing multiplicities of infection (m.o.i. = 3, 10, 30, and 100) of Ad encoding FLAG-

tagged NEU1 and cultured for 48 h. In selected experiments, cells infected with Ad-NEU1 (m.o.i. = 100) were transfected with either NEU1-targeting or control siRNAs. In still other experiments, Ad-infected cells (m.o.i. = 100) were incubated for 15 min with EGF (100 ng/ml) or medium alone. The cells were solubilized with a low stringency lysis buffer as described (28), and the lysates were precleared and then incubated overnight at 4 °C with anti-EGFR or anti-MUC1 antibody. The resultant immune complexes were immobilized by incubation with protein G-agarose for 2 h at 4 °C, centrifuged, washed, boiled for 7 min in sample buffer, and again centrifuged. The supernatants were processed for immunoblotting with anti-FLAG antibody as described above. To control for loading and transfer of immunoprecipitates, blots were stripped and reprobed with the immunoprecipitating antibodies. Each FLAG signal was normalized to either the EGFR or MUC1 signal in the same lane in the same blot.

*Lectin Blotting for Sialylated and Desialylated Molecules*—A549 cells were transfected with NEU1-targeting or control siRNAs and incubated for 48 h or infected with Ad-NEU1 or Ad-Null (m.o.i. = 100) and incubated for 24 h. The cells were solubilized with lysis buffer as described above, and 1.0-mg aliquots were immunoprecipitated with anti-EGFR, anti-MUC1, or anti-TLR5 antibody. Immunoprecipitated proteins were resolved by SDS-PAGE and transferred to PVDF membrane. The blots were incubated for 1 h in TBS-T and probed with biotinylated MAL or PNA as described (24). The blots were washed with TBS-T, incubated with HRP-conjugated streptavidin, and developed with ECL reagents. Fetuin and asialofetuin (1.0 $\mu$g each) were used as positive controls for MAL-binding and PNA-binding proteins, respectively. To confirm equivalent protein loading and transfer, blots were stripped and reprobed with the immunoprecipitating antibody followed by HRP-conjugated secondary antibody and ECL reagents.

*EGFR Activation*—SAECs and A549 cells were transfected with NEU1-targeting or control siRNAs or infected with Ad-NEU1 or Ad-Null (m.o.i. = 100) after which they were incubated for 10 min with 100 ng/ml EGF or medium alone. The ECs were lysed, and the lysates were processed for phospho-EGFR (Tyr-1068), total EGFR, and $\beta$-tubulin immunoblotting as described (29). The phospho-EGFR blots were stripped and reprobed for total EGFR and $\beta$-tubulin, and the phospho-EGFR Tyr-1068 signal was normalized to $\beta$-tubulin in the same lane of the same gel.

*Bacterial Adhesion*—SAECs and A549 cells were transfected with NEU1-targeting or control siRNAs and incubated for 48 h or infected with Ad-NEU1 or Ad-Null (m.o.i. = 100) and incubated for 24 h. The cells were washed twice with PBS, fixed for 10 min with 2.5% glutaraldehyde in PBS at room temperature, and washed three times with PBS as described (30). Green fluorescent protein-expressing *Pseudomonas aeruginosa* strain PA01 (GFP-PA01) provided by Dr. Joanna B. Goldberg (University of Virginia, Charlottesville, VA) (31) was cultured overnight in LB broth, washed twice with PBS, resuspended in PBS containing 2.0 mg/ml glucose, and quantified spectrophotometrically at $A_{600}$. Fixed cells ($2.0 \times 10^5$/well) in 24-well plates were incubated with $2.0 \times 10^7$ colony-forming units/well of GFP-PA01 in 0.5 ml for 40 min at 37 °C and washed three times

with PBS. Bound bacteria were released with 0.05% trypsin, and GFP fluorescence in the supernatant was quantified with a fluorometer (excitation, 490 nm; emission, 520 nm) (Bio-Rad). In other experiments, A549 cells in which NEU1 expression was similarly manipulated were transfected with MUC1-targeting or control siRNAs and incubated for 24 h prior to the bacterial adhesion assay.

*Purification of P. aeruginosa Flagellin*—An overnight culture of *P. aeruginosa* was centrifuged at $5,000 \times g$ for 30 min, resuspended in Krebs-Ringer buffer, and incubated for 1 h at 37 °C as described (32). The bacteria were removed by centrifugation, and the supernatant was filtered through a 0.22-$\mu$m-pore membrane (Millipore) and boiled for 20 min. The supernatant was concentrated by ultrafiltration (Millipore; 30-kDa cutoff), adjusted to pH 6.0, and incubated for 30 min at room temperature with 0.5 ml of Macro-Prep High S support, pH 6.0. The matrix was removed by centrifugation, and the flagellin-containing supernatant was applied to a 2.0-ml Macro-Prep High Q column. The column was washed with 20 mM Tris-HCl, pH 8.0, and flagellin was eluted with 100 ml of a linear 0.0–1.0 M NaCl gradient. Fractions (1.0 ml) were collected and analyzed for the 50-kDa flagellin protein band by SDS-PAGE. Immunoblots were probed with rabbit anti-*P. aeruginosa* flagellin antibody (provided by Dr. Dan Wozniak, Wake Forest University, Winston-Salem, NC) and with rabbit anti-pilin antibody (provided by Dr. Randy Irvin, University of Alberta, Alberta, Canada) to confirm the absence of pilin contamination. Flagellin-containing fractions were adsorbed to polymyxin B-agarose to remove LPS after which less than 0.1 endotoxin units/$\mu$g of protein was detected by the *Limulus* amebocyte lysate test.

*MUC1 Signaling*—SAECs and A549 cells were transfected with NEU1-targeting or control siRNAs or infected with Ad-NEU1 or Ad-Null (m.o.i. = 100). The cells were incubated for 30 min at 37 °C with 10 ng/ml flagellin or medium alone and lysed, and the lysates were processed for phospho-ERK1/2 immunoblotting as described (33). The phospho-ERK1/2 blots were stripped and reprobed for total ERK2, and the phospho-ERK1/2 signal was normalized to total ERK2 signal in the same lane of the same gel.

*Immunostaining of NEU1 in Human Tissues*—Human trachea, mainstem bronchus, segmented bronchus, and expanded alveoli were each obtained from ≥2 normal subjects through an Institutional Review Board-approved protocol at the University of Maryland, Baltimore, MD. The sections were deparaffinized in xylene and rehydrated in a graded series of ethanol. Sections were pretreated for heat-induced epitope retrieval using a pressure cooker and Target Retrieval solution, pH 6.1 (Dako TRS, S1699/1700) followed by endogenous peroxidase blocking for 5 min with 0.3% hydrogen peroxide. The sections were incubated overnight with anti-NEU1 antibody at a 1:250 dilution at 4 °C in a hydration chamber. Antibody detection was performed by incubation with biotinylated goat anti-rabbit secondary antibody for 30 min at room temperature. Slides were developed for 5 min using diaminobenzidine as the chromogen (Dako) and counterstained with hematoxylin. As a negative control, tissue sections were incubated with non-immune rabbit IgG plus the secondary antibody. Staining was performed on a Dako automatic stainer using EnVision+ (Dako), a biotin-free detection system that consists of a secondary antibody covalently linked to peroxidase-coated dextrose polymers.

*Statistical Analysis*—All values were expressed as means ± S.E. Differences between means were compared using the Student's *t* test or analysis of variance and were considered significant at $p < 0.05$.

## RESULTS

*Airway EC Sialidase Activity*—Respiratory epithelial surfaces express multiple glycoconjugates that are terminally sialylated (2, 3). We asked whether airway epithelia might also express sialidase activity. Increasing alveolar A549 EC and primary SAEC numbers expressed increasing sialidase activity for the fluorogenic substrate 4-MU-NANA (Fig. 1*A*). This sialidase activity was destroyed by boiling and was dose-dependently inhibited by the substrate-competitive sialidase inhibitor 2-deoxy-NANA but not by its negative control, 2-keto-3-deoxyoctulosonic acid (Fig. 1*B*). Purified *N*-acetylneuraminic acid also was dose-dependently inhibitory (Fig. 1*C*). ECs derived from human trachea, bronchus, small airways, and the alveolus all contained sialidase activity for 4-MU-NANA (Fig. 1*D*). To our knowledge, this is the first report of sialidase activity in human airway epithelia.

*EC Expression of NEU1, -2, -3, and -4 and Cathepsin A*—Because airway ECs contain sialidase activity (Fig. 1, *A* and *D*), we asked whether one or more of the four reported mammalian sialidases might be expressed in these same cells. In primary SAECs, a qRT-PCR approach was adopted to detect mRNAs for NEU1, -2, -3, and -4. NEU1 mRNA was expressed at the highest level, $380 \pm 5.0 \times 10^{-3}$ copies relative to expression of the hypoxanthine-guanine phosphoribosyltransferase internal control (Fig. 2*A*). In contrast, the mRNAs for NEU2, -3, and -4 were expressed at $0.05 \pm 0.001 \times 10^{-3}$, $0.65 \pm 0.050 \times 10^{-3}$, and $0.09 \pm 0.002 \times 10^{-3}$ copies, respectively, relative to hypoxanthine-guanine phosphoribosyltransferase. Therefore, at the mRNA level, NEU1 was expressed at levels 585–7,600-fold higher than were NEU2, -3, and -4. We then used an antibody specific for the NEU1 protein to probe lysates of A549 cells and SAECs. NEU1 was detected as a doublet at ~45 and ~50 kDa (Fig. 2*B*, *lanes 1* and *2*). The lower band corresponded to the predicted molecular size of NEU1 based upon its cDNA sequence, 45.5 kDa (27). The upper band may represent glycosylation at one or more of its three predicted *N*-linked sites (27). Prior siRNA-induced silencing reduced the intensity of both bands (Fig. 2*B*, *lane 3*), whereas a non-targeting control siRNA did not (supplemental Fig. S1*B, lanes 1, 3, and 5*). These findings clearly indicate that NEU1 protein is expressed in both A549 cells and SAECs. Because ECs derived from the trachea and bronchus contain sialidase activity against 4-MU-NANA (Fig. 1*D*), these same cells were probed for NEU1 protein. All airway epithelia examined expressed both the ~45-kDa and ~50-kDa NEU1-immunoreactive bands (Fig. 2*C*). Because NEU1 requires cathepsin A for catalytic activity (20), these same airway epithelia were probed for cathepsin A protein with a monoclonal antibody that recognizes the 52-kDa full-length form and the 32-kDa processed fragment (Fig. 2*D*). Again, all airway epithelia studied expressed both cathepsin A-immuno-
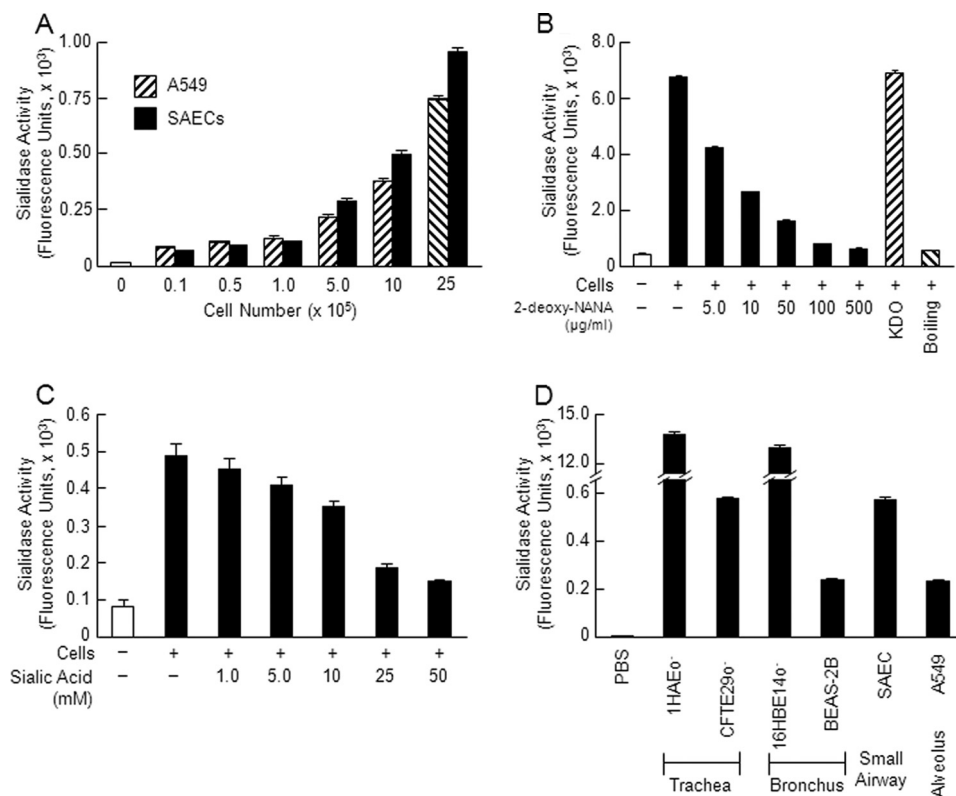
FIGURE 1. **EC sialidase activity.** *A*, increasing SAEC and A549 cell numbers were assayed for sialidase activity for the fluorogenic substrate 4-MU-NANA. *B*, A549 cells ($1.0 \times 10^6$) were assayed for sialidase activity for 4-MU-NANA prior to and after boiling and in the presence of increasing concentrations of 2-deoxy-NANA (5–500 $\mu$g/ml) or its negative control, 2-keto-3-deoxyoctulosonic acid (*KDO*) (500 $\mu$g/ml). *C*, A549 cells ($1.0 \times 10^6$) were assayed for 4-MU-NANA in the presence of increasing concentrations of *N*-acetylneuraminic acid (1–50 mM). *D*, equal numbers of airway ECs ($1.0 \times 10^6$) derived from the trachea (1HAEo⁻ and CFTE29o⁻), bronchus (16HBE14o⁻ and BEAS-2B), small airways (SAECs), and alveolus (A549) or PBS as a negative control was assayed for sialidase activity for the 4-MU-NANA substrate. *Vertical* and *error bars* represent mean $\pm$ S.E. sialidase activity ($n \geq 2$) expressed as arbitrary fluorescence units. The results in each panel represent $\geq 2$ independent experiments.

reactive bands. These combined data suggest that NEU1 and cathepsin A are co-expressed along the entire respiratory tract.

*NEU1 Sialidase Activity*—On the basis of qRT-PCR (Fig. 2*A*) and Western (Fig. 2, *B* and *C*) analyses, we asked whether EC-associated sialidase activity might be explained in part through NEU1. To unambiguously establish siRNA-induced knock-down of NEU1, FLAG-tagged NEU1 was ectopically expressed in A549 cells through Ad infection (supplemental Fig. S1*A*). A549 cells overexpressing NEU1 were transfected with NEU1-targeting or control siRNAs after which the cells were lysed, and the lysates were processed for FLAG immunoblotting. At 24 and 48 h, NEU1 was reduced >95% relative to control siRNA-transfected cells (supplemental Fig. S1*B, lane 2 versus lane 1* and *lane 4 versus lane 3*). To exclude off-target effects, A549 cells overexpressing HA-tagged NEU3 were transfected with NEU1-targeting, NEU3-targeting, or control siRNAs and lysed, and the lysates were processed for HA immunoblotting. At 48 h, NEU3 in cells transfected with NEU3-targeting siRNAs was profoundly reduced (supplemental Fig. S1*C, lane 2 versus lane 1*), whereas in cells transfected with NEU1-targeting siRNAs, it was not (supplemental Fig. S1*C, lane 3 versus lane 1*), each relative to control siRNA-transfected cells. Therefore, NEU1-targeting siRNA did not diminish NEU3 protein, indicating both efficient and selective siRNA-induced depletion of NEU1 in A549 cells. Next, to establish the contribution of NEU1 to sialidase activity in airway ECs, A549 cells transfected

with NEU1-targeting or control siRNAs after 48 h were fluoro-metrically assayed for sialidase activity. Prior siRNA-mediated knockdown of NEU1 decreased sialidase activity for 4-MU-NANA by >70% compared with control siRNA-transfected cells (Fig. 2*E*). Because NEU3, the second most abundant EC sialidase at the mRNA level (Fig. 2*A*), preferentially hydrolyzes SA linkages within gangliosides (17), we assayed A549 cells and SAECs for sialidase activity using a ganglioside substrate. Each expressed sialidase activity for gangliosides (Fig. 2*F*). Therefore, it is conceivable that the residual sialidase activity detected in airway epithelia after NEU1 depletion is due in part to NEU3. The catalytic activity of NEU1 or NEU3 for a specific substrate is dictated by the SA linkage, the underlying glycan, the presence of detergent, and pH (27). Although NEU1 and NEU3 display distinct substrate specificities, under certain conditions, NEU1 might exert catalytic activity for gangliosides, whereas NEU3 may hydrolyze SA residues within the 4-MU-NANA substrate (17, 34).

*Subcellular Localization of NEU1*—Because NEU1 has been previously immunolocalized in non-airway cells to specific subcellular compartments (35), we utilized confocal fluorescence microscopy to probe for NEU1 protein. A549 cells revealed granular/punctate immunostaining for NEU1 with maximal signal in the perinuclear region (Fig. 2*G, panel i*). NEU1 was not detected within nuclei (Fig. 2*G, panel ii, arrows*). NEU1 is a lysosomal protein (20, 48). To establish whether NEU1 resides

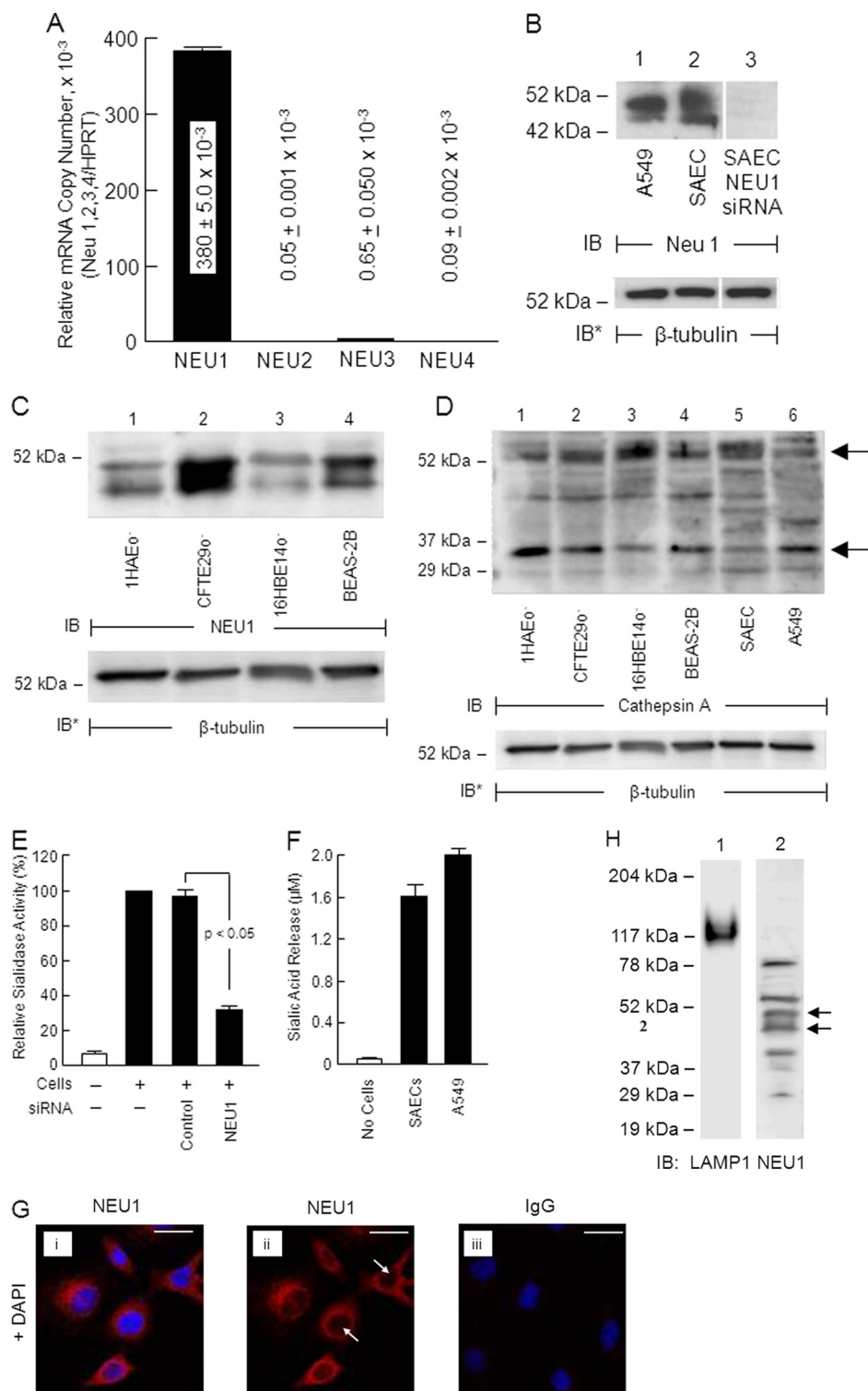# NEU1 Regulates EGFR and MUC1 Signaling in Airway Epithelia



FIGURE 2. **Expression of NEU1 in airway ECs.** *A*, qRT-PCR analyses of NEU1, NEU2, NEU3, and NEU4 transcripts. The mRNA levels for each sialidase were normalized to the hypoxanthine-guanine phosphoribosyltransferase (*HPRT*) internal control. *Vertical* and *error bars* represent mean ± S.E. normalized mRNA levels ($n = 2$). *B*, lysates of A549 cells and SAECs were processed for NEU1 immunoblotting (*lanes 1* and *2*). SAECs were transfected with NEU1-targeting siRNAs and processed for NEU1 immunoblotting (*lane 3*). *C*, lysates of airway ECs were processed for NEU1 immunoblotting. *D*, lysates of airway ECs were processed for cathepsin A immunoblotting. *Arrows* indicate the 52-kDa full-length and the 32-kDa processed cathepsin A-immunoreactive bands. In *B*, *C*, and *D*, to control for protein loading and transfer, blots were stripped and reprobed for β-tubulin. *IB*, immunoblot; *IB\**, immunoblot after stripping. Molecular mass in kDa is indicated on the *left*. Each blot is representative of ≥3 independent experiments. *E*, after transfection with NEU1-targeting or control siRNAs, A549 cells were assayed for sialidase activity for the 4-MU-NANA substrate. *F*, SAECs and A549 cells ($1.0 \times 10^6$) were assayed for sialidase activity for the bovine brain ganglioside substrate. *Vertical* and *error bars* represent mean ± S.E. sialidase activity expressed as arbitrary fluorescence units (*E*) ($n = 5$) or SA release (*F*) ($n = 2$). *G*, subconfluent A549 cells were probed with anti-NEU1 antibody (*panels i* and *ii*) or non-immune IgG as a negative control (*panel iii*) and counterstained with DAPI (overlays in *panels i* and *iii*). *Arrows* indicate the nuclear regions in NEU1-stained cells in the absence of DAPI (*panel ii*). *Scale bar*, 25 μm. Each photomicrograph is representative of ≥2 independent experiments. *H*, lysosomal preparations isolated from A549 cells were processed for immunoblotting with antibodies raised against LAMP1 (*lane 1*) and NEU1 (*lane 2*). *IB*, immunoblot. Molecular mass in kDa is indicated on the *left*. *Arrows* on the *right* indicate the NEU1-immunoreactive bands of interest.
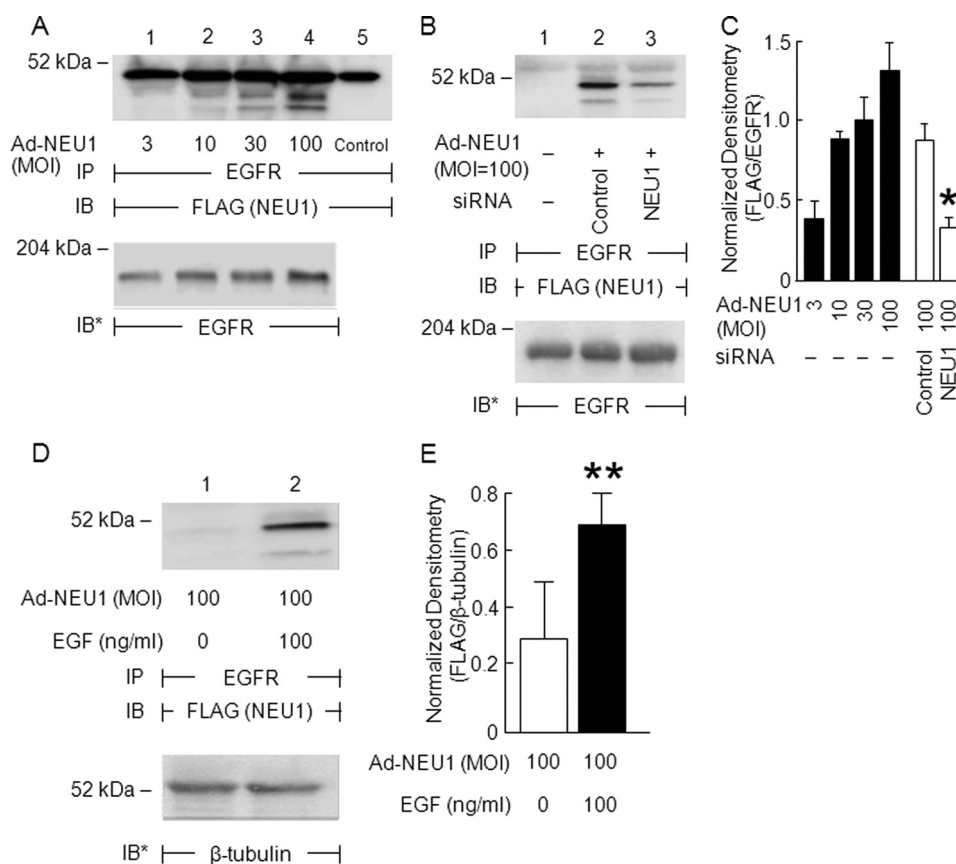
FIGURE 3. **NEU1 associates with EGFR in airway ECs.** *A*, A549 cells were infected with increasing multiplicities of infection of Ad-NEU1 and after 48 h were lysed, and the lysates were immunoprecipitated with anti-EGFR antibody. In *lane 5*, the antibody alone was introduced to control for Ig heavy chain. *B*, A549 cells infected with Ad-NEU1 (m.o.i. = 100) were transfected with NEU1-targeting or control siRNAs after which they were lysed, and the lysates were immunoprecipitated with anti-EGFR antibody. *D*, A549 cells infected with Ad-NEU1 (m.o.i. = 100) were incubated for 15 min with EGF (100 ng/ml) or medium alone and lysed, and the lysates were immunoprecipitated with anti-EGFR antibody. In *A*, *B*, and *D*, the EGFR immunoprecipitates were processed for FLAG tag immunoblotting. To control for loading and transfer of immunoprecipitates, blots were stripped and reprobed with anti-EGFR antibody. *IP*, immunoprecipitation; *IB*, immunoblot; *IB\**, immunoblot after stripping. Molecular mass in kDa is indicated on the *left*. Each blot is representative of three independent experiments. The densitometric analyses of the blots in *A* and *B* are presented in *C*, and the densitometric analyses of the blots in *D* are presented in *E*. *Vertical* and *error bars* represent mean ± S.E. FLAG signal normalized to EGFR signal in the same lane on the same blot (*n* = 3). \*, significantly decreased FLAG/EGFR densitometry of cells transfected with NEU1-targeting *versus* control siRNAs at *p* < 0.05. \*\*, significantly increased FLAG/EGFR densitometry of EGF-stimulated *versus* medium control cells at *p* < 0.05.

within the lysosomal compartment of airway epithelia, lysosomal preparations isolated from A549 cells were processed for immunoblotting with antibodies raised against NEU1 and the lysosomal marker LAMP1 (Fig. 2*H*). A 117–120-kDa LAMP1-immunoreactive band was clearly detected, validating the A549-derived preparation as enriched for lysosomal proteins (Fig. 2*H*, *lane 1*). When this same preparation was probed for NEU1 protein, a NEU1-reactive doublet that migrated with molecular masses of ∼45 and ∼50-kDa was seen (Fig. 2*H*, *lane 2*). These combined studies establish the presence of a relatively abundant intracellular pool of NEU1 that in A549 cells can be immunodetected at least in part in lysosomes.

*Association of NEU1 with EGFR*—Because NEU1 is known to associate with multiple receptor signaling complexes (36–40), we asked whether NEU1 might also associate with EGFR. Ad-NEU1 infection with multiplicities of infection of ≥10 dose-dependently increased NEU1 co-immunoprecipitation with EGFR (Fig. 3, *A* and *C*). Conversely, prior knockdown of NEU1 diminished NEU1 co-immunoprecipitation with EGFR compared with that seen in control siRNA-transfected cells (Fig. 3, *B* and *C*). We then asked whether EGF stimulation might alter

the NEU1-EGFR interaction. EGF increased NEU1 co-immunoprecipitation with EGFR (Fig. 3, *D* and *E*). These combined data indicate that NEU1 associates with EGFR and that the NEU1-EGFR interaction is regulated by EGF stimulation.

*EGFR Is an in Vivo NEU1 Substrate*—EGFR is central to the airway EC migratory response and repair program (1, 29). EGFR itself is sialylated (6), its sialylation state regulates receptor dimerization and activation (41), and its response to ligands can be influenced by gangliosides (7, 8). We now have demonstrated that NEU1 associates with EGFR (Fig. 3). To determine whether NEU1 regulates EGFR activation, we first asked whether EGFR might be an *in vivo* substrate for NEU1. In A549 cells in which NEU1 was either silenced (supplemental Fig. S1*B*) or overexpressed (supplemental Fig. S1*A*), EGFR immunoprecipitates were processed for lectin blotting with MAL, which recognizes terminal SA residues in α-2,3 linkages (42), or PNA, which recognizes subterminal galactose residues that become accessible after removal of terminal SA (43). Prior knockdown of NEU1 increased MAL binding to EGFR compared with the control siRNA-transfected cells (Fig. 4*A*, *lane 2 versus lane 1*). In contrast, NEU1 overexpression diminished MAL binding to EGFR com-
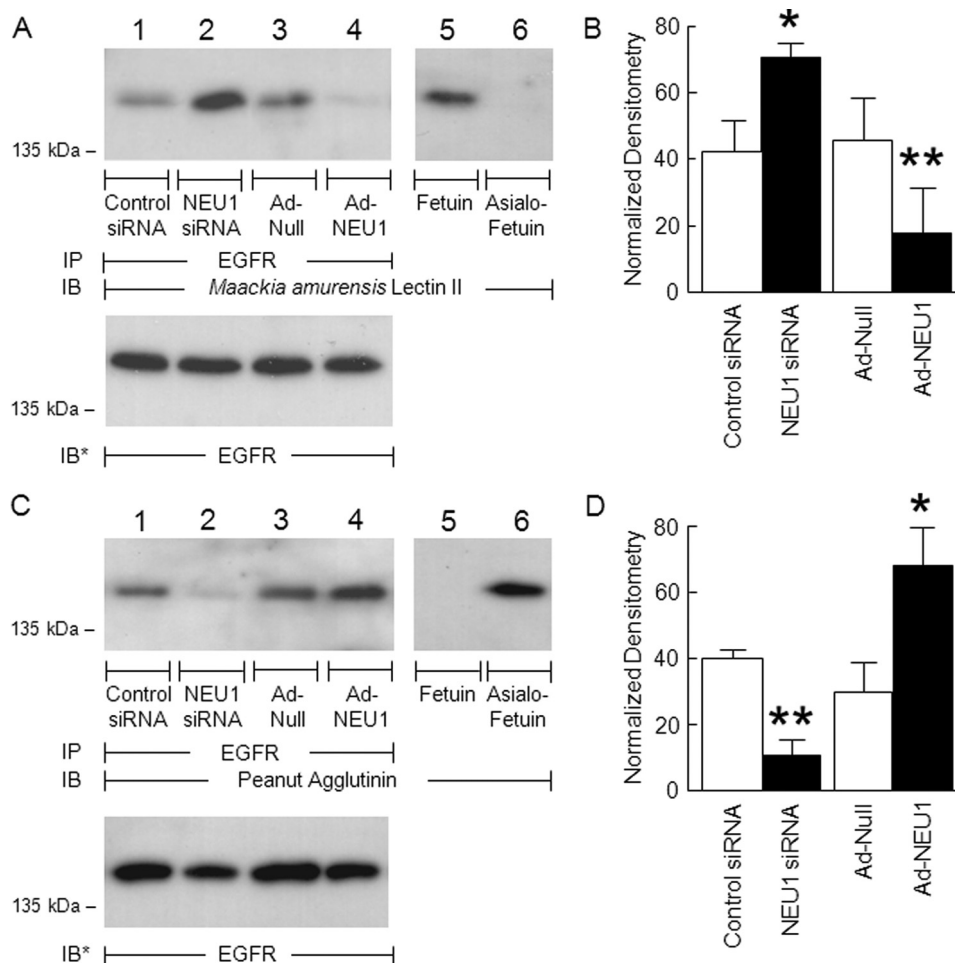
FIGURE 4. **EGFR is NEU1 substrate in airway ECs.** A549 cells were transfected with NEU1-targeting or control siRNAs or infected with Ad-NEU1 or Ad-Null at an m.o.i. of 100. Cell lysates were immunoprecipitated with anti-EGFR antibody. The EGFR immunoprecipitates were resolved by SDS-PAGE and probed with MAL (*A*) or PNA (*C*). As controls for lectin specificity, parallel blots of fetuin and asialofetuin were simultaneously probed (*lanes 5* and *6*). To control for protein loading and transfer, blots were stripped and reprobed with anti-EGFR antibody. *IP*, immunoprecipitation; *IB*, immunoblot; *IB\**, immunoblot after stripping. Molecular mass in kDa is indicated on the *left*. Each blot is representative of two independent experiments. The densitometric analyses of the blots in *A* and *C* are presented in *B* and *D*, respectively. *Vertical* and *error bars* represent mean $\pm$ S.E. MAL/PNA signal normalized to EGFR signal in the same lane on the same blot ($n = 2$). \*, significantly increased lectin/EGFR densitometry of NEU1 siRNA- or Ad-NEU1-treated cells compared with control siRNA- or Ad-Null-treated cells at $p < 0.05$. \*\*, significantly decreased lectin/EGFR densitometry of NEU1 siRNA- or Ad-NEU1-treated cells compared with control siRNA- or Ad-Null-treated cells at $p < 0.05$.

pared with Ad-Null-infected cells (Fig. 4*A*, *lane 4 versus lane 3*). When each MAL binding signal was normalized to the total EGFR signal in the same lane in the same gel, silencing of NEU1 increased detection of SA in EGFR by 1.7-fold, whereas NEU1 overexpression decreased detection of SA in EGFR by 60% (Fig. 4*B*). Conversely, when comparable samples were probed with PNA lectin to detect EGFR desialylation, knockdown of NEU1 decreased PNA signal compared with control siRNA-transfected cells (Fig. 4*C*, *lane 2 versus lane 1*), and NEU1 overexpression increased PNA signal compared with Ad-Null-infected cells (Fig. 4*C*, *lane 4 versus lane 3*). Densitometric analysis of the PNA lectin blots indicated that NEU1 knockdown diminished detection of terminal galactose by 73%, whereas NEU1 overexpression enhanced the PNA signal by 2.3-fold (Fig. 4*D*). These combined data indicate that in airway epithelia NEU1 cleaves SA residues from EGFR. To be catalytically active, NEU1 must operate within a multiprotein complex comprising NEU1, cathepsin A, and $\beta$-galactosidase (19, 44). In those experiments where NEU1 alone was overexpressed, our results may be understated.

*NEU1 Regulates EGFR Activation*—Because NEU1 associates with EGFR (Fig. 3) and EGFR is an *in vivo* substrate for NEU1 (Fig. 4), we next asked whether NEU1 might regulate ligand-dependent EGFR autophosphorylation. In A549 cells in which NEU1 was either silenced or overexpressed, EGF-stimulated EGFR Tyr-1068 phosphorylation was studied. In preliminary experiments, total EGFR was profoundly diminished following EGF stimulation irrespective of NEU1 manipulation (supplemental Fig. S2, *A* and *C, lanes 2* and *4*) likely due to ligand-dependent endocytosis and degradation of EGF-EGFR complexes (45). Accordingly, the phospho-Tyr-1068 EGFR signal was normalized to $\beta$-tubulin expression. Under all experimental conditions examined, EGF consistently increased EGFR Tyr-1068 phosphorylation compared with the simultaneous medium control (Fig. 5*A*, *C*, and *E, lanes 2 versus lane 1* and *lane 4 versus lane 3*). Prior knockdown of NEU1 followed by EGF treatment enhanced the phospho-Tyr-1068 signal compared with EGF-treated, control siRNA-transfected cells (Fig. 5*A*, *lane 4 versus lane 2*). In contrast, in both A549 cells and SAECs,
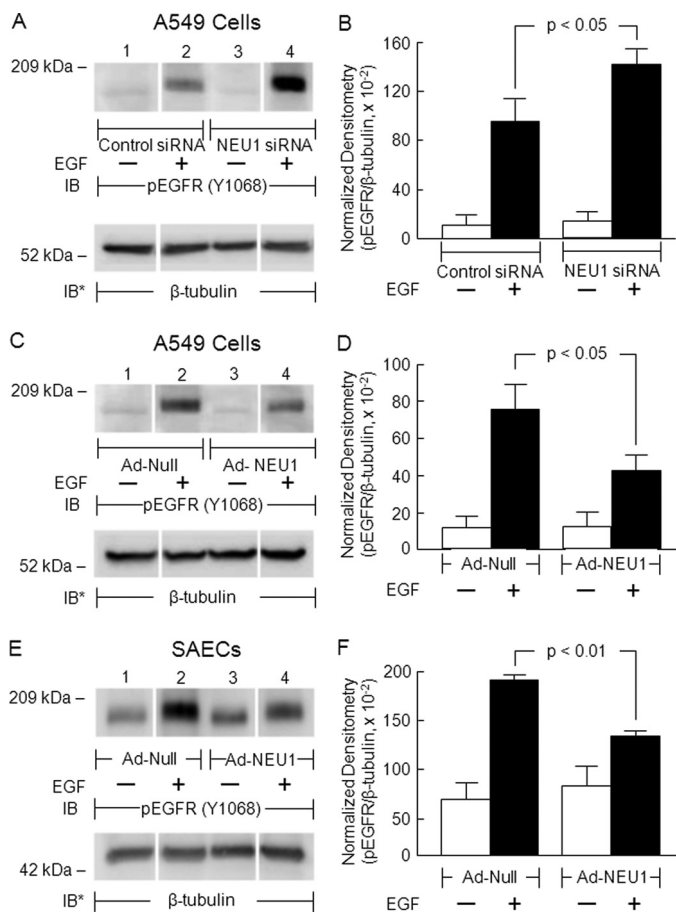
**FIGURE 5. NEU1 regulates EGFR activation in airway ECs.** A549 cells (*A* and *C*) or SAECs (*E*) were transfected with NEU1-targeting or control siRNAs or infected with Ad-NEU1 or Ad-Null at an m.o.i. of 100. The cells were treated with EGF or medium alone, and cell lysates were processed for phospho-EGFR (Tyr-1068) immunoblotting. To control for protein loading and transfer, blots were stripped and reprobed for $\beta$-tubulin. *IB*, immunoblot; *IB\**, immunoblot after stripping. Molecular mass in kDa is indicated on the *left*. Each blot is representative of two independent experiments. The densitometric analyses of the blots in *A*, *C*, and *E* are presented in *B*, *D*, and *F*, respectively. *Vertical* and *error bars* represent mean ± S.E. phospho-EGFR (*pEGFR*) signal normalized to $\beta$-tubulin signal in the same lane on the same blot (*n* = 2).

NEU1 overexpression diminished the phospho-Tyr-1068 signal in response to EGF compared with EGF-treated, Ad-Null-infected cells (Fig. 5, *C* and *E*, lane 4 versus lane 2). Densitometric analyses indicated that NEU1 knockdown increased EGF-stimulated Tyr-1068 phosphorylation by 1.5-fold in A549 cells (Fig. 5*B*), whereas NEU1 overexpression decreased phosphorylation by 44% in A549 cells (Fig. 5*D*) and by 32% in SAECs (Fig. 5*F*). Taken together, these data suggest that NEU1-mediated desialylation of EGFR diminishes its autophosphorylation on Tyr-1068 in response to the EGF stimulus. Whether NEU1 targets SA residues within the ligand-binding portion of the EGFR ectodomain to influence the receptor-ligand interaction, regulates EGFR homo/heterodimerization, and/or alters EGFR responsiveness to inhibitory gangliosides is unknown.

*Association of NEU1 with MUC1*—Because we now have demonstrated that NEU1 associates with EGFR (Fig. 3) and EGFR is known to physically interact with MUC1 (10), we asked whether NEU1 might also associate with MUC1. Ad-NEU1 infection with multiplicities of infection of ≥10 dose-dependently increased NEU1 co-immunoprecipitation with MUC1

(supplemental Fig. S3, *A* and *B*). In contrast, prior NEU1 depletion decreased NEU1 co-immunoprecipitation with MUC1 compared with control siRNA-transfected cells (supplemental Fig. S3, *C* and *D*). These results indicate that NEU1 constitutively associates with MUC1. Whether NEU1 directly associates with MUC1 or does so indirectly via EGFR is unclear.

*MUC1 Is an in Vivo NEU1 Substrate*—MUC1 is a heavily sialylated, membrane-bound glycoprotein that influences a diverse range of host cell activities, including EC interactions with pathogens and intracellular signal transduction (9). We now have demonstrated that NEU1 associates with MUC1 (supplemental Fig. S3). To determine whether NEU1 might also regulate MUC1 function, we first asked whether this membrane-tethered mucin might be an *in vivo* substrate for NEU1. In A549 cells in which NEU1 was either silenced or overexpressed, MUC1 immunoprecipitates were processed for lectin blotting with MAL or PNA. Prior knockdown of NEU1 increased MAL binding compared with the control siRNA-transfected cells (Fig. 6*A*, lane 2 versus lane 1), whereas NEU1 overexpression diminished MAL binding compared with Ad-Null-infected cells (Fig. 6*A*, lane 4 versus lane 3). When each MAL signal was normalized to total MUC1 signal, silencing of NEU1 increased detection of SA in MUC1 by 1.6-fold, whereas NEU1 overexpression decreased detection of SA by 80% (Fig. 6*B*). Conversely, when identical samples were probed with PNA to detect MUC1 desialylation, knockdown of NEU1 decreased the PNA signal compared with control siRNA-transfected cells (Fig. 6*C*, lane 2 versus lane 1), and NEU1 overexpression increased PNA binding compared with Ad-Null-infected cells (Fig. 6*C*, lane 4 versus lane 3). Densitometric analysis of the PNA lectin blots indicated that NEU1 knockdown diminishes MUC1 desialylation by 62%, whereas NEU1 overexpression enhanced desialylation by 1.5-fold (Fig. 6*D*). These combined data indicate that in airway epithelia NEU1 cleaves SA residues from MUC1. In contrast, neither $\alpha$-2,3-linked terminal SA or galactose residues were detected on TLR5 (supplemental Fig. S4), a distinct surface-expressed glycoprotein that like MUC1 also recognizes and responds to bacterial flagellin (11, 12).

*NEU1 Regulates MUC1-mediated Bacterial Adhesion*—Because MUC1 is an *in vivo* substrate for NEU1 (Fig. 6) and is known to bind to *P. aeruginosa* (30, 46), we asked whether NEU1 might regulate MUC1-dependent bacterial adhesion to airway ECs. In A549 cells or SAECs in which NEU1 was either silenced or overexpressed, *P. aeruginosa* binding was studied. Prior knockdown of NEU1 diminished bacterial adhesion by 38% in A549 cells compared with control siRNA-transfected cells (Fig. 7*A*), whereas NEU1 overexpression enhanced bacterial adhesion by 1.6-fold in A549 cells (Fig. 7*B*) and by 1.7-fold in SAECs (Fig. 7*C*) compared with Ad-Null-infected cells. In contrast, NEU3 overexpression in A549 cells did not alter bacterial adhesion compared with Ad-Null-infected cells (Fig. 7*B*). To confirm that bacterial adhesion was mediated through MUC1, *P. aeruginosa* binding was studied in A549 cells in which NEU1 expression was silenced or overexpressed as well as transfected with MUC1-targeting or control siRNAs. Transfection with MUC1-targeting siRNAs reduced MUC1 protein to undetectable levels (supplemental Fig. S5) as described pre-
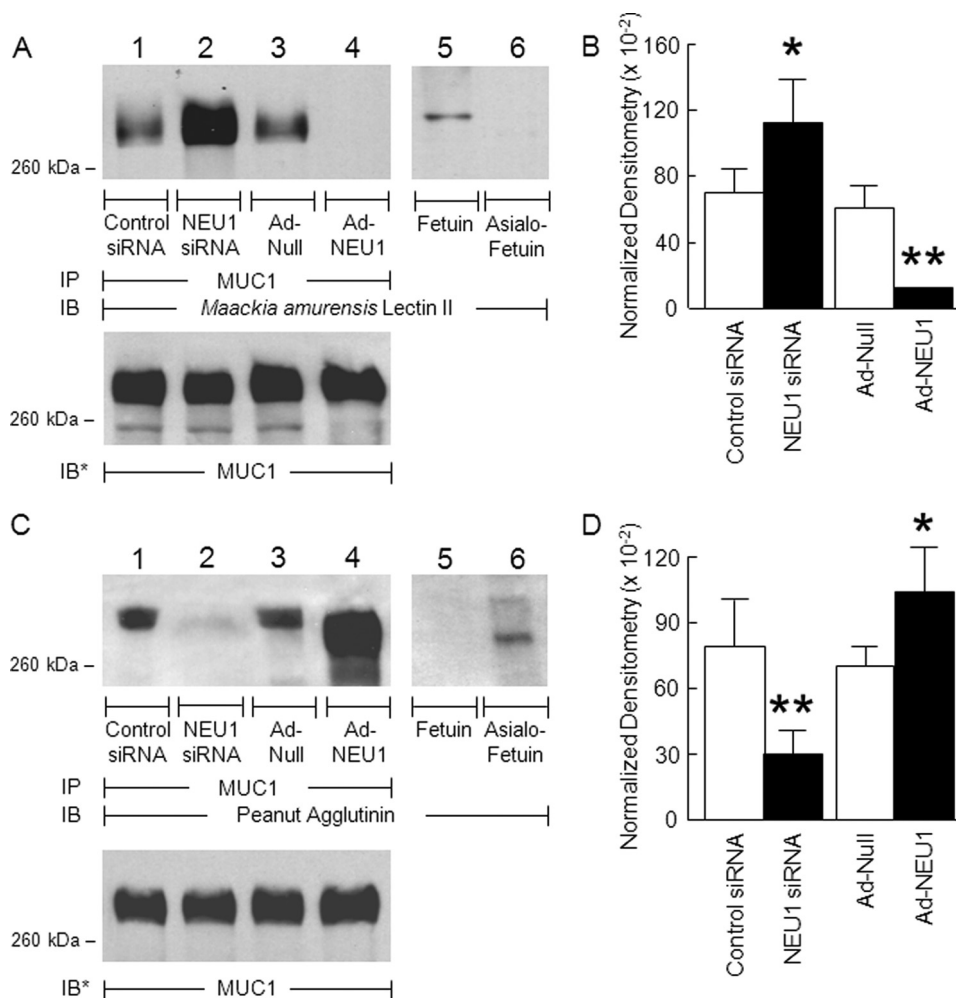
FIGURE 6. **MUC1 is NEU1 substrate in airway ECs.** *A*, A549 cells were transfected with NEU1-targeting or control siRNAs or infected with Ad-NEU1 or Ad-Null at an m.o.i. of 100. Cell lysates were immunoprecipitated with anti-MUC1 antibody. Immunoprecipitated proteins were processed for lectin blotting with MAL (*A*) or PNA (*C*). As a control for lectin specificity, parallel blots of fetuin and asialofetuin were simultaneously probed (*lanes 5* and *6*). To control for protein loading and transfer, blots were stripped and reprobed with anti-MUC1 antibody. *IP*, immunoprecipitation; *IB*, immunoblot; *IB\**, immunoblot after stripping. Molecular mass in kDa is indicated on the *left*. Each blot is representative of two independent experiments. The densitometric analyses of the lectin blots in *A* and *C* are presented in *B* and *D*, respectively. *Vertical* and *error bars* represent mean ± S.E. normalized densitometry values (*n* = 2). *, significantly increased lectin/MUC1 densitometry of NEU1 siRNA- or Ad-NEU1-treated cells compared with control siRNA- or Ad-Null-treated cells at $p < 0.05$. **, significantly decreased lectin/ MUC1 densitometry of NEU1 siRNA- or Ad-NEU1-treated cells compared with control siRNA- or Ad-Null-treated cells at $p < 0.05$.

viously (25). When these same experiments were performed in A549 cells in which MUC1 had been silenced, no differences in bacterial adhesion to NEU1-targeting *versus* control siRNA-transfected cells (Fig. 7*D*) or to Ad-NEU1-infected cells *versus* Ad-Null-infected cells (Fig. 7*E*) were observed. In contrast, MUC1-expressing cells exhibited 56% reduced adhesion after NEU1 knockdown (Fig. 7*D*) and 2.0-fold increased adhesion after NEU1 overexpression (Fig. 7*E*). These data indicate that *P. aeruginosa* directly or indirectly binds to MUC1 and that the MUC1 sialylation state influences its bacterial adhesiveness.

*NEU1 Regulates MUC1-coupled Signaling*—Because manipulation of NEU1 expression altered the sialylation state of MUC1 (Fig. 6) and *P. aeruginosa* adhesion to MUC1-expressing cells (Fig. 7), we next asked whether NEU1 might regulate MUC1-dependent downstream signal transduction. In A549 cells or SAECs in which NEU1 was either silenced or overexpressed, flagellin-stimulated, MUC1-dependent ERK1/2 phosphorylation was studied as described previously (33). In MUC1-expressing ECs, *P. aeruginosa*-derived flagellin consistently

increased ERK1/2 phosphorylation compared with the simultaneous medium control (Fig. 8*A*, *C*, *E*, and *G*, *lanes 2 versus lane 1* and *lane 4 versus lane 3*). Prior knockdown of NEU1 followed by flagellin treatment diminished flagellin-stimulated ERK1/2 phosphorylation compared with flagellin-treated, control siRNA-transfected cells (Fig. 8*A*, *lane 4 versus lane 2*). In both A549 cells and SAECs, NEU1 overexpression enhanced the phospho-ERK1/2 signal in response to flagellin compared with flagellin-treated, Ad-Null-infected cells (Fig. 8, *C* and *E*, *lanes 4 versus lane 2*). Densitometric analyses indicated that NEU1 knockdown decreased flagellin-stimulated ERK1/2 phosphorylation by 73% in A549 cells (Fig. 8*B*), whereas NEU1 overexpression increased the phospho-ERK1/2 signal by 1.9-fold in A549 cells (Fig. 8*D*) and by 1.7-fold in SAECs (Fig. 8*F*). Finally, although NEU1 overexpression in control siRNA-transfected, MUC1-expressing A549 cells increased the phospho-ERK1/2 signal by 1.7-fold in response to flagellin compared with flagellin-treated, Ad-Null-infected cells (Fig. 8*G*, *lane 4 versus lane 2*), no increase in ERK1/2 activation was seen
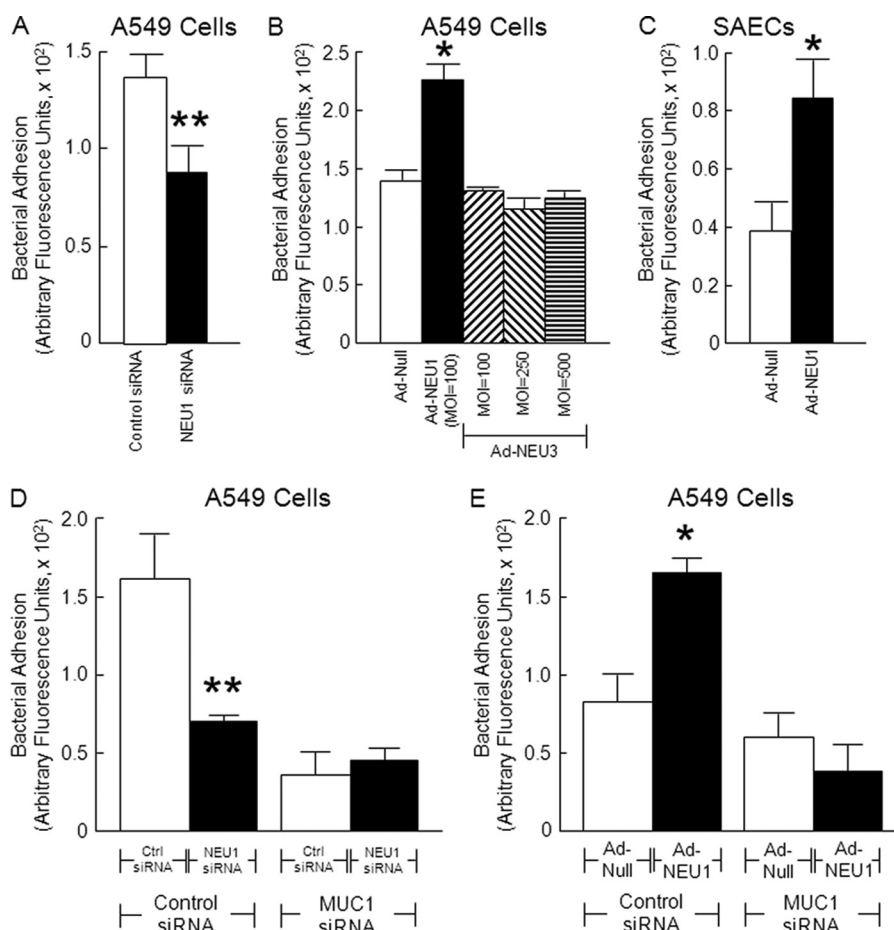
FIGURE 7. **NEU1 regulates bacterial adhesion to airway ECs.** A549 cells (*A* and *B*) or SAECs (*C*) were transfected with NEU1-targeting or control siRNAs or infected with Ad-NEU1 or Ad-Null at an m.o.i. of 100. In selected experiments, A549 cells were infected with Ad-NEU3 at multiplicities of infection of 100, 250, and 500 (*B*). The cells were fixed, washed, and incubated with GFP-PA01. Unbound bacteria were removed by washing, bound bacteria were released with 0.05% trypsin, and GFP in the supernatant was fluorometrically quantified. *D* and *E*, A549 cells in which NEU1 was manipulated were transfected with MUC1-targeting or control (*Ctrl*) siRNAs, and bacterial adhesion was assayed. *Vertical* and *error bars* represent mean ± S.E. arbitrary fluorescence units (*n* = 4). *, significantly increased bacterial adhesion to Ad-NEU1- compared with Ad-Null-infected cells at $p < 0.05$. **, significantly decreased bacterial adhesion to NEU1 siRNA-transfected *versus* control siRNA-transfected cells at $p < 0.05$.

in NEU1-overexpressing cells transfected with the MUC1 siRNA (Fig. 8*H*, *lane 4 versus lane 2*). Densitometric analyses of the blots generated in Fig. 8, *G* and *H*, are displayed in Fig. 8*I*. Taken together, these data indicate that NEU1-mediated desialylation of MUC1 increases not only bacterial adhesion (Fig. 7) but also flagellin-stimulated ERK1/2 phosphorylation. That prior MUC1 depletion abrogated the response to flagellin is consistent with a MUC1-mediated, TLR5-independent process.

*NEU1 Immunostaining in Airway Epithelia in Human Tissues*—Sialidase activity can be detected in cultured ECs derived from various portions of the human airway (Fig. 1*D*), and NEU1 protein is expressed in these same epithelia (Fig. 2, *B* and *C*). We asked whether NEU1 protein expression could be extended to normal intact human tissues. In the trachea, intense NEU1 staining was evident at the mucosal surface (Fig. 9*A*). This epithelial staining was intense in the cytoplasm with relative sparing of nuclei (Fig. 9*A*, *inset, arrow*). The subepithelial mesenchymal cells displayed diminished staining relative to epithelia. In the mainstem bronchus, NEU1 staining was most intense in the superficial portion of the epithelial cytoplasm, including the brush border (Fig. 9*B*). Here, the subepithelial mesenchymal cells were weakly stained. In the segmented

bronchi, strong cytoplasmic staining was evident in the epithelial cell layer, whereas again, the subepithelial mesenchyma was stained weakly (Fig. 9*C*). Anthracotic pigment was apparent and is not to be confused with NEU1 staining (Fig. 9*C*, *arrowheads*). In the expanded alveoli, the epithelial cells contained both cytoplasmic and nuclear staining (Fig. 9*D*, *inset, arrow*). Sections probed with a species- and isotype-matched, non-immune control IgG were completely non-reactive (Fig. 9*E*). In those hematoxylin-stained tissues where NEU1 appeared to localize to the nucleus, it likely represented cytoplasmic staining superimposed over the nucleus as supported by our confocal microscopic studies (Fig. 2*G*, *panel ii*). Therefore, NEU1 protein was expressed in airway epithelia, especially within the brush border, but not in subepithelial tissues. Clear differences between the distributions of NEU1 protein along the length of the human lower airway were not evident.

## DISCUSSION

We now have demonstrated sialidase activity in respiratory airway epithelia (Figs. 1, *A*, and *D*, and 2*E*). The EC-associated sialidase activity could be detected in the presence of 4-MU-NANA substrate, was heat-labile (Fig. 1*B*), and was dose-de-
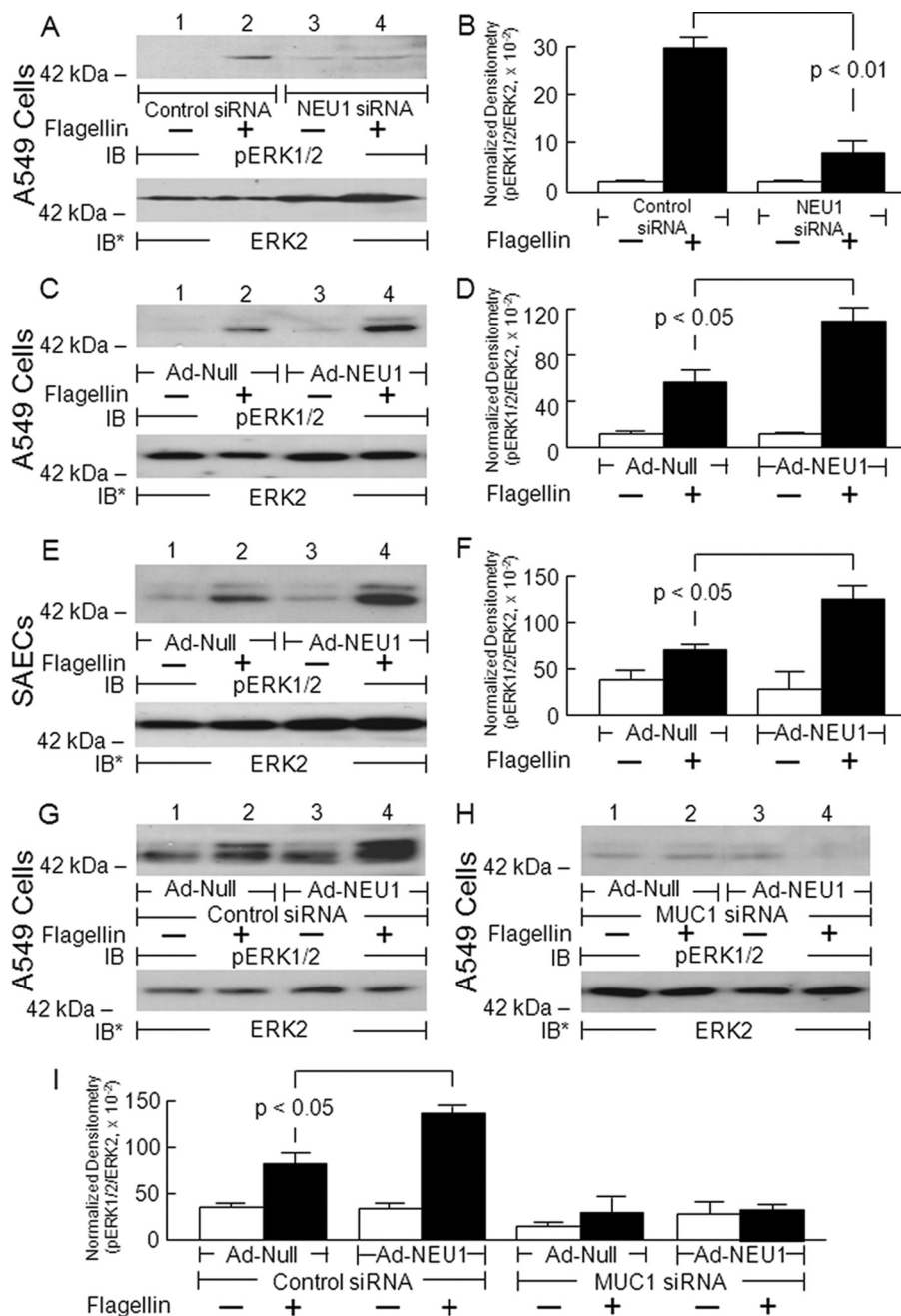
FIGURE 8. **NEU1 regulates flagellin-stimulated ERK1/2 activation in airway ECs.** A549 cells (*A* and *C*) or SAECs (*E*) were transfected with NEU1-targeting or control siRNAs or infected with Ad-NEU1 or Ad-Null at an m.o.i. of 100. The cells were treated with *P. aeruginosa* flagellin or medium alone. Cell lysates were processed for phospho-ERK1/2 immunoblotting. *G* and *H*, A549 cells infected with Ad-NEU1 or Ad-Null were transfected with MUC1-targeting (*H*) or control (*G*) siRNAs, treated with flagellin or medium alone, and processed for phospho-ERK1/2 (*pERK1/2*) immunoblotting. To control for protein loading and transfer, blots were stripped and reprobed with anti-ERK2 antibody. *IB*, immunoblot; *IB\**, immunoblot after stripping. Molecular mass in kDa is indicated on the *left*. Each blot is representative of two independent experiments. The densitometric analyses of the blots in *A*, *C*, *E*, *G*, and *H* are presented in *B*, *D*, *F*, and *I*, respectively. *Vertical* and *error bars* represent mean ± S.E. normalized densitometry values (*n* = 2).

pendently inhibited by purified *N*-acetylneuraminic acid (Fig. 1*C*) and the sialidase inhibitor 2-deoxy-NANA but not by its negative control, 2-keto-3-deoxyoctulosonic acid (Fig. 1*B*). In SAECs, NEU1 mRNA was expressed at far greater levels than were mRNAs for NEU2, NEU3, or NEU4 (Fig. 2*A*). At the protein level, NEU1 and cathepsin A were detected in ECs derived from trachea, bronchus, small airways, and alveoli (Fig. 2, *B*, *C*, and *D*). Prior siRNA-induced knockdown of NEU1 diminished sialidase activity in the 4-MU-NANA assay by >70% (Fig. 2*E*).

Using confocal fluorescence microscopy, an intracellular pool of NEU1 could be immunolocalized to the perinuclear region (Fig. 2*G*) and could be detected in lysosomal preparations (Fig. 2*H*). In co-immunoprecipitation assays, NEU1 associated with both EGFR (Fig. 3, *A–C*) and MUC1 (supplemental Fig. S3, *A–C*); the NEU1-EGFR association was regulated by EGF stimulation (Fig. 3, *D* and *E*). On the basis of MAL and PNA lectin blotting, EGFR and MUC1 were established as *in vivo* substrates for NEU1. NEU1 overexpression desialylated these two
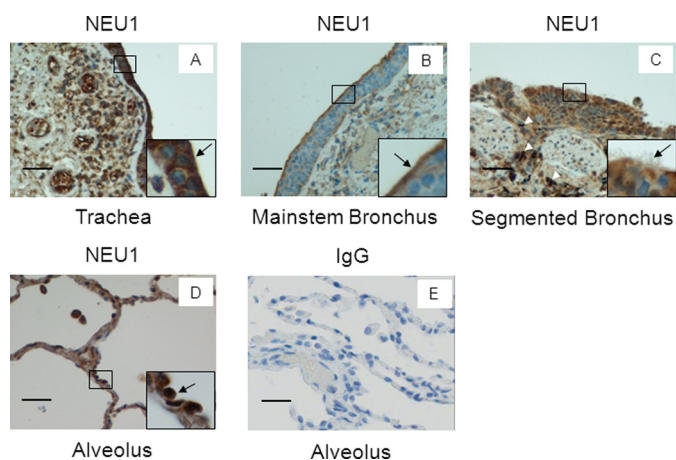
FIGURE 9. **NEU1 immunostaining of airway epithelia in human tissues.** Sections of human tissues were processed for NEU1 immunohistochemistry. *A*, trachea; *B*, mainstem bronchus; *C*, segmented bronchus; *D*, expanded alveoli. *E*, as a negative control, sections of alveoli were probed with non-immune rabbit IgG. Each section was photographed at 400× or 1,000× (*insets*). *Scale bar*, 50 μm. *Arrows* indicate immunostaining for NEU1. *Arrowheads* indicate anthracotic pigment. Each photograph is representative of two sections.

receptors, whereas silencing of NEU1 increased their sialylation states (Figs. 4 and 6). NEU1 depletion enhanced EGFR Tyr-1068 phosphorylation (Fig. 5, *A* and *B*), whereas NEU1 overexpression diminished it (Fig. 5, *C–F*). In contrast, silencing of NEU1 decreased both *P. aeruginosa* adhesion (Fig. 7, *A* and *D*) and flagellin-induced ERK 1/2 activation (Fig. 8, *A* and *B*), whereas its overexpression increased these two MUC1-mediated events (Figs. 7, *B*, *C*, and *E*, and 8, *C–I*). To be catalytically active, NEU1 must operate within a multiprotein complex comprising NEU1, cathepsin A, and β-galactosidase (19, 20, 29). In those experiments where NEU1 alone was overexpressed, it is possible that our results are understated. Finally, NEU1 was detected in human tissues, including trachea, mainstem and segmented bronchi, and alveoli, almost exclusively in the superficial epithelium (Fig. 9, *A–D*).

NEU1 has been localized to lysosomes where its catalytic activity requires its close association with cathepsin A and β-galactosidase (19, 20). However, we now have demonstrated that NEU1 clearly can desialylate surface structures, such as EGFR (Fig. 4) and MUC1 (Fig. 6). Although the mechanisms through which NEU1 might be translocated to the plasma membrane are poorly understood, it has been detected on the surface of multiple cell types (47–49). A tyrosine-containing internalization motif in the COOH terminus of NEU1, amino acids 412–415, reportedly targets the enzyme to the lysosome in COS-7 cells, human skin fibroblasts, and lymphocytes (48). Upon NEU1 Tyr-412 phosphorylation in activated lymphocytes, NEU1 is redistributed to the cell surface (48). In other studies, NEU1 was targeted to the plasma membrane of phorbol 12-myristate 13-acetate-differentiated human monocytes (47) and activated human T lymphocytes (49). In each case, NEU1 was accompanied by cathepsin A. NEU1 activation has been coupled to ligand engagement of TLR4 (36), the elastin receptor complex (37, 38), and Trk A (39). In addition to EGFR (Fig. 4) and MUC1 (Fig. 6), NEU1 has also been shown to desialylate TLR4 (36) and the receptors for platelet-derived growth factor-BB and insulin growth factor (40). These combined data

indicate that NEU1 can be strategically co-localized in close proximity to surface receptor substrates.

The EGFR ectodomain contains 12 potential *N*-linked glycosylation sites, a portion of which are glycosylated and terminally sialylated (6). Five potential *N*-glycosylation sites and >500 potential *O*-linked sites are located in the MUC1 extracellular domain of which 70–90% of the latter are terminally sialylated (9). In our lectin blotting studies, MAL and PNA recognized EGFR (Fig. 4, *A* and *C*) and MUC1 (Fig. 6, *A* and *C*) immunoprecipitates, indicating co-expression of α-2,3-linked SA and β-D-galactose in the absence of NEU1 manipulation. In the case of MUC1, prior lectin blotting studies have demonstrated co-reactivity with MAL and PNA, thus confirming the presence of both residues (50, 51). After NEU1-mediated desialylation, recognition of EGFR and MUC1 by PNA was increased (Figs. 4*C*, *lane 4*, and 6*C*, *lane 4*), indicating that the removed SA residues were linked to penultimate β-D-galactose. NEU1 expression at supraphysiological levels might indiscriminately desialylate one or more sialylated proteins expressed on the EC surface. However, NEU1 depletion profoundly increased the sialylation states of both glycoproteins (Figs. 4*A*, *lane 2*, and 6*A*, *lane 2*). This latter finding would indicate that in unstimulated, resting ECs constitutive NEU1-mediated desialylation occurs. This ongoing desialylation could maintain an altered threshold for EGFR activation (Fig. 5) or for the MUC1 response to pathogenic bacteria (Figs. 7 and 8).

EGFR is sialylated (6), and its sialylation state regulates its dimerization and autophosphorylation (41). Because SA linkages on EGFR can be hydrolyzed by NEU1 (Fig. 4), we asked whether NEU1 might regulate ligand-dependent EGFR activation. We found that NEU1 overexpression diminished EGFR Tyr-1068 phosphorylation in response to EGF (Fig. 5, *C–F*), whereas NEU1 depletion had the opposite effect (Fig. 5, *A* and *B*). These findings suggest that SA is required for optimal EGFR responsiveness and/or that removal of SA residues permits recognition of an inhibitory stimulus. EGFR activation is regulated in part by gangliosides (7, 8). In epithelia, GM3 is the predominant ganglioside (52). In A431 cells, GM3 directly interacts with *N*-linked glycans in the EGFR ectodomain to inhibit both ligand-dependent and ligand-independent EGFR dimerization and autophosphorylation without altering ligand binding (52). Furthermore, the GM3 inhibitory effect could be enhanced by prior neuraminidase treatment (7). GM3 appeared to counter-regulate phosphorylation of EGFR Tyr-845, Tyr-1068, and Tyr-1148 but not Tyr-1086 or Tyr-1173 (52). Similarly, in our studies, NEU1 overexpression diminished EGF-stimulated EGFR Tyr-1068 phosphorylation (Fig. 5, *C–F*). Therefore, it is conceivable that NEU1 desialylates the terminally sialylated *N*-linked oligosaccharides to which GM3 binds in the EGFR ectodomain, thereby promoting the GM3-EGFR interaction and GM3-mediated attenuation of EGFR activation. However, NEU1 might also desialylate gangliosides themselves, including GM3 (34), potentially influencing receptor-ligand and/or receptor-receptor interactions. Interestingly, another sialidase, NEU3, is localized within the plasma membrane and preferentially hydrolyzes ganglioside substrates (17, 53). In response to EGF, NEU3 is redistributed to ruffling cell membranes where it co-localizes with and activates RAC1 and increases cell motility

(54). Whether NEU1 regulates the sialylation state of the EGFR ectodomain in concert with NEU3 and/or other sialidases is unknown.

An initial adhesion step by mucosal pathogens to host epithelia is essential for establishment of infection (55). In the airways, multiple EC binding sites for *P. aeruginosa* have been described (56–60), including, in our own studies, MUC1 (30, 46). We found that binding of *P. aeruginosa* to MUC1 was mediated through flagellin (32), and the flagellin-MUC1 interaction was coupled to ERK1/2 activation (33). In the current studies, we now have demonstrated that the same NEU1 overexpression that diminished the sialylation state of MUC1 (Fig. 6*A*, *lane 4*) and at the same time unmasked subterminal β-D-galactose residues (Fig. 6*C*, *lane 4*) also increased *P. aeruginosa* binding to A549 cells and SAECs (Fig. 7, *B* and *C*). Similarly, pretreatment of A549 cells with *Salmonella typhimurium*-derived neuraminidase increased *P. aeruginosa* adhesion by 2.0-fold compared with untreated cells (61). Conversely, prior NEU1 depletion, which increased MUC1 sialylation (Fig. 6*A*, *lane 2*) and at the same time diminished access to β-D-galactose sites (Fig. 6*C*, *lane 2*), reduced *P. aeruginosa* adhesion (Fig. 7*A*). Finally, prior silencing of MUC1 totally eliminated all changes in *P. aeruginosa* adhesion associated with manipulation of NEU1 expression (Fig. 7, *D* and *E*). These combined data indicate that NEU1 regulates the sialylation state of MUC1, which in turn controls its adhesiveness to *P. aeruginosa*. Residual bacterial binding to A549 cells in the absence of MUC1 expression likely represents adhesion to one or more of the other airway EC surface receptors cited above. Interestingly, one of these receptors, asialo-GM1, also mediates *P. aeruginosa* adhesion as a non-sialylated moiety (56, 60). More recently, MUC1 has been established as an adhesion molecule for bacterial pathogens other than *P. aeruginosa* (62–64). Whether NEU1 might also regulate binding of other bacteria to MUC1 is unknown.

*P. aeruginosa* adheres to MUC1 (Fig. 7) and through flagellin stimulates ERK1/2 signaling in epithelia (Fig. 8) (32, 33). Because MUC1 is both a receptor for flagellin and an *in vivo* substrate for NEU1, we asked whether NEU1 might regulate ERK1/2 activation in response to *P. aeruginosa*-derived flagellin. We found that NEU1 overexpression, which desialylates MUC1 (Fig. 6*A*, *lane 4*) and unmasks subterminal β-D-galactose sites (Fig. 6*C*, *lane 4*), enhanced flagellin-induced ERK1/2 phosphorylation (Fig. 8, *C–F*). Conversely, prior silencing of NEU1, which increased MUC1 sialylation (Fig. 6*A*, *lane 2*) and decreased detection of β-D-galactose sites (Fig. 6*C*, *lane 2*), attenuated ERK1/2 activation in response to the flagellin stimulus (Fig. 8, *A* and *B*). Several possible mechanisms may underlie these observations. First, terminal SA may mask one or more flagellin recognition sites within the MUC1 ectodomain. Second, the MUC1 recognition motif for flagellin binding may comprise subterminal galactose residues. Third, the enhanced EC response to flagellin following desialylation might be explained in part through an intermediary galactose-binding component, such as galectin-3 (57). Finally, NEU1-mediated desialylation of MUC1 may regulate its association with TLR5, an established co-receptor for flagellin (11).

SA residues can either mask recognition motifs or actively participate in the recognition process itself (3, 65). In the case of EGFR, prior desialylation diminished the EGFR response to EGF (Fig. 5, *C–F*). Either SA is required for this receptor-ligand interaction, or desialylation plays a permissive role for an inhibitory stimulus, such as GM3 (52, 66). In the case of MUC1, prior desialylation increased both *P. aeruginosa* adhesion (Fig. 7, *B* and *C*) and flagellin-stimulated ERK1/2 activation (Fig. 8, *C–F*). Here, the SA appears to mask the recognition site(s) for *P. aeruginosa* and its flagellin. The role that NEU1-mediated desialylation might play in EGFR and MUC1 activation is further complicated by their cooperativity (10). MUC1 interacts with EGFR, and activated EGFR tyrosine phosphorylates the MUC1 cytoplasmic domain at a -YEKV- motif that upon phosphorylation serves as a docking site for the c-Src SH2 domain (67). MUC1 also protects against EGFR ubiquitination, thereby promoting its postinternalization plasma membrane recycling and signaling (68). The net effect of NEU1-mediated desialylation on the EGFR-MUC1 receptor signaling complex is likely complicated and incompletely understood. Evidence exists to support the concept that NEU1 can regulate the responsiveness of other receptors in addition to EGFR and MUC1. Endotoxin engagement of TLR4 is coupled to NEU1 activation and desialylation of the TLR4 ectodomain, permitting TLR4 dimerization and activation (36, 69). The elastin receptor complex comprises three subunits, including elastin-binding protein, a spliced variant of lysosomal β-galactosidase, cathepsin A, and NEU1 (37, 38). Elastase-generated elastin peptides bind to the receptor complex to up-regulate NEU1 activity. Whether NEU1 might regulate these same receptors within the airways requires further study.

The sialylation state of secreted glycoproteins, receptors, and the cell surface influences protein-protein, receptor-ligand, and cell-cell interactions, which in turn regulate developmental programs, tissue morphogenesis, wound healing, and tumor cell biology (2, 3). Whether the NEU1 sialidase offers an additional level of control over these SA-driven processes and whether these regulatory mechanisms are operative within the airway are less clear. Genetic mutations in the human *NEU1* locus lead to the lysosomal storage disease sialidosis (70). Sialidosis patients with the early onset form of the disease have a mucopolysaccharidosis-like phenotype with a subset of cases presenting with respiratory complications (71). In Neu1$^{-/-}$ mice, normal alveolar wall septation does not occur, resulting in enlarged alveoli that are maintained in adults due to the requirement of Neu1 for normal assembly of elastic fibers (72). These combined studies suggest that NEU1 is required for normal lung development and function. Although the NEU1 promoter has been characterized and potential regulatory elements have been defined (73), few stimuli for its up-regulation have been identified. During phorbol ester-induced monocyte differentiation, *NEU1* gene expression is up-regulated (47). IL-1 stimulation of human neutrophils increases NEU1 transcript levels ~3-fold (34). Ligand engagement of TLR2, -3, and -4 with zymosan, poly(I-C), and lipopolysaccharide, respectively, (69) and binding of elastin peptides to the elastin receptor complex (58) both reportedly increase NEU1 activity. That EGFR has now been established as an *in vivo* NEU1 substrate (Fig. 4) implicates NEU1 in airway epithelial repair and wound healing, tumorigenesis, and metastatic potential (1, 74). In fact,

NEU1 overexpression has been reported to suppress anchorage-independent growth and metastasis of murine B16 melanoma cells (75) and human colon cancer cells (76). Because NEU1 desialylates MUC1 (Fig. 6), it may regulate mucus viscosity and mucociliary clearance. In response to inflammatory and septic processes within the lung, such as tracheobronchitis or pneumonia, numerous innate immune pathways, many of which are tightly regulated through sialylation/desialylation, are activated. The initial pathogen-EC interaction for selected viruses, bacteria, and their toxins is SA-dependent (3). We found that NEU1-mediated desialylation dramatically enhanced adhesion of *P. aeruginosa* to airway epithelia (Fig. 7, *B* and *C*). Whether NEU1 can hydrolyze the SA linkages expressed in the capsules or lipopolysaccharide of prokaryotes is unclear. Through its ability to modify one or more TLRs (36, 69) or adhesion molecules (76), NEU1 may regulate proinflammatory gene expression and leukocyte trafficking (23, 24). NEU1 may also influence recruitment of inflammatory cells into the bronchoalveolar compartment through the generation of complement cleavage products (77) and altered binding of antibodies to the Fc receptor (78), which in turn may alter opsonic activity in bronchoalveolar fluids for recruited granulocytes and/or resident alveolar macrophages. Finally, transepithelial migration of leukocytes and overall epithelial barrier integrity might be further controlled by NEU1 through its ability to reorganize sialylated E-cadherin to open the paracellular pathway (79, 80). NEU1, possibly in concert with one or more other sialidase(s), likely offers an additional level of regulation over multiple airway epithelial responses to ligands, inflammatory cells, and injurious stimuli.

## REFERENCES

1. Burgel, P. R., and Nadel, J. A. (2004) Roles of epidermal growth factor receptor activation in epithelial cell repair and mucin production in airway epithelium. *Thorax* **59,** 992–996
2. Varki, A. (2008) Sialic acids in human health and disease. *Trends Mol. Med.* **14,** 351–360
3. Schauer, R. (2009) Sialic acids as regulators of molecular and cellular interactions. *Curr. Opin. Struct. Biol.* **19,** 507–514
4. Gagneux, P., Cheriyan, M., Hurtado-Ziola, N., van der Linden, E. C., Anderson, D., McClure, H., Varki, A., and Varki, N. M. (2003) Human-specific regulation of $\alpha$2–6-linked sialic acids. *J. Biol. Chem.* **278,** 48245–48250
5. Rose, M. C., and Voynow, J. A. (2006) Respiratory tract mucin genes and mucin glycoproteins in health and disease. *Physiol. Rev.* **86,** 245–278
6. Yoon, S. J., Nakayama, K., Hikita, T., Handa, K., and Hakomori, S. I. (2006) Epidermal growth factor receptor tyrosine kinase is modulated by GM3 interaction with *N*-linked GlcNAc termini of the receptor. *Proc. Natl. Acad. Sci. U.S.A.* **103,** 18987–18991
7. Kawashima, N., Yoon, S. J., Itoh, K., and Nakayama, K. (2009) Tyrosine kinase activity of epidermal growth factor receptor is regulated by GM3 binding through carbohydrate to carbohydrate interactions. *J. Biol. Chem.* **284,** 6147–6155
8. Li, R., Liu, Y., and Ladisch, S. (2001) Enhancement of epidermal growth factor signaling and activation of SRC kinase by gangliosides. *J. Biol. Chem.* **276,** 42782–42792
9. Hattrup, C. L., and Gendler, S. J. (2008) Structure and function of the cell surface (tethered) mucins. *Annu. Rev. Physiol.* **70,** 431–457
10. Schroeder, J. A., Thompson, M. C., Gardner, M. M., and Gendler, S. J. (2001) Transgenic MUC1 interacts with epidermal growth factor receptor and correlates with mitogen-activated protein kinase activation in the mouse mammary gland. *J. Biol. Chem.* **276,** 13057–13064
11. Hayashi, F., Smith, K. D., Ozinsky, A., Hawn, T. R., Yi, E. C., Goodlett, D. R., Eng, J. K., Akira, S., Underhill, D. M., and Aderem, A. (2001) The innate immune response to bacterial flagellin is mediated by Toll-like receptor 5. *Nature* **410,** 1099–1103
12. Adamo, R., Sokol, S., Soong, G., Gomez, M. I., and Prince, A. (2004) *Pseudomonas aeruginosa* flagella activate airway epithelial cells through asialoGM1 and toll-like receptor 2 as well as toll-like receptor 5. *Am. J. Respir. Cell Mol. Biol.* **30,** 627–634
13. Imberty, A., and Varrot, A. (2008) Microbial recognition of human cell surface glycoconjugates. *Curr. Opin. Struct. Biol.* **18,** 567–576
14. Trappetti, C., Kadioglu, A., Carter, M., Hayre, J., Iannelli, F., Pozzi, G., Andrew, P. W., and Oggioni, M. R. (2009) Sialic acid: a preventable signal for pneumococcal biofilm formation, colonization, and invasion of the host. *J. Infect. Dis.* **199,** 1497–1505
15. Harduin-Lepers, A., Vallejo-Ruiz, V., Krzewinski-Recchi, M. A., Samyn-Petit, B., Julien, S., and Delannoy, P. (2001) The human sialyltransferase family. *Biochimie* **83,** 727–737
16. Monti, E., Preti, A., Venerando, B., and Borsani, G. (2002) Recent development in mammalian sialidase molecular biology. *Neurochem. Res.* **27,** 649–663
17. Miyagi, T., Wada, T., Iwamatsu, A., Hata, K., Yoshikawa, Y., Tokuyama, S., and Sawada, M. (1999) Molecular cloning and characterization of a plasma membrane-associated sialidase specific for gangliosides. *J. Biol. Chem.* **274,** 5004–5011
18. Monti, E., Preti, A., Nesti, C., Ballabio, A., and Borsani, G. (1999) Expression of a novel human sialidase encoded by the NEU2 gene. *Glycobiology* **9,** 1313–1321
19. Pshezhetsky, A. V., Richard, C., Michaud, L., Igdoura, S., Wang, S., Elsliger, M. A., Qu, J., Leclerc, D., Gravel, R., Dallaire, L., and Potier, M. (1997) Cloning, expression and chromosomal mapping of human lysosomal sialidase and characterization of mutations in sialidosis. *Nat. Genet.* **15,** 316–320
20. Bonten, E. J., and d'Azzo, A. (2000) Lysosomal neuraminidase. Catalytic activation in insect cells is controlled by the protective protein/cathepsin A. *J. Biol. Chem.* **275,** 37657–37663
21. Comelli, E. M., Amado, M., Lustig, S. R., and Paulson, J. C. (2003) Identification and expression of Neu4, a novel murine sialidase. *Gene* **321,** 155–161
22. Hyun, S. W., Anglin, I. E., Liu, A., Yang, S., Sorkin, J. D., Lillehoj, E., Tonks, N. K., Passaniti, A., and Goldblum, S. E. (2011) Diverse injurious stimuli reduce protein tyrosine phosphatase-$\mu$ expression and enhance epidermal growth factor receptor signaling in human airway epithelia. *Exp. Lung Res.* **37,** 327–343
23. Cross, A. S., Sakarya, S., Rifat, S., Held, T. K., Drysdale, B. E., Grange, P. A., Cassels, F. J., Wang, L. X., Stamatos, N., Farese, A., Casey, D., Powell, J., Bhattacharjee, A. K., Kleinberg, M., and Goldblum, S. E. (2003) Recruitment of murine neutrophils *in vivo* through endogenous sialidase activity. *J. Biol. Chem.* **278,** 4112–4120
24. Sakarya, S., Rifat, S., Zhou, J., Bannerman, D. D., Stamatos, N. M., Cross, A. S., and Goldblum, S. E. (2004) Mobilization of neutrophil sialidase activity desialylates the pulmonary vascular endothelial surface and increases resting neutrophil adhesion to and migration across the endothelium. *Glycobiology* **14,** 481–494
25. Guang, W., Ding, H., Czinn, S. J., Kim, K. C., Blanchard, T. G., and Lillehoj, E. P. (2010) Muc1 cell surface mucin attenuates epithelial inflammation in response to a common mucosal pathogen. *J. Biol. Chem.* **285,** 20547–20557
26. Gong, P., Angelini, D. J., Yang, S., Xia, G., Cross, A. S., Mann, D., Bannerman, D. D., Vogel, S. N., and Goldblum, S. E. (2008) TLR4 signaling is coupled to SRC family kinase activation, tyrosine phosphorylation of zonula adherens proteins, and opening of the paracellular pathway in human lung microvascular endothelia. *J. Biol. Chem.* **283,** 13437–13449
27. Achyuthan, K. E., and Achyuthan A. M. (2001) Comparative enzymology, biochemistry and pathophysiology of human exo-$\alpha$-sialidases

(neuraminidases). *Comp. Biochem. Physiol. B Biochem. Mol. Biol.* **129,** 29–64

28. Angelini, D. J., Hyun, S. W., Grigoryev, D. N., Garg, P., Gong, P., Singh, I. S., Passaniti, A., Hasday, J. D., and Goldblum, S. E. (2006) TNF-α increases tyrosine phosphorylation of vascular endothelial cadherin and opens the paracellular pathway through fyn activation in human lung endothelia. *Am. J. Physiol. Lung Cell. Mol. Physiol.* **291,** L1232–L1245

29. Liu, A., Garg, P., Yang, S., Gong, P., Pallero, M. A., Annis, D. S., Liu, Y., Passaniti, A., Mann, D., Mosher, D. F., Murphy-Ullrich, J. E., and Goldblum, S. E. (2009) Epidermal growth factor-like repeats of thrombospondins activate phospholipase Cγ and increase epithelial cell migration through indirect epidermal growth factor receptor activation. *J. Biol. Chem.* **284,** 6389–6402

30. Lillehoj, E. P., Hyun, S. W., Kim, B. T., Zhang, X. G., Lee, D. I., Rowland, S., and Kim, K. C. (2001) Muc1 mucins on the cell surface are adhesion sites for *Pseudomonas aeruginosa. Am. J. Physiol. Lung Cell. Mol. Physiol.* **280,** L181–L187

31. Lindorfer, M. A., Nardin, A., Foley, P. L., Solga, M. D., Bankovich, A. J., Martin, E. N., Henderson, A. L., Price, C. W., Gyimesi, E., Wozencraft, C. P., Goldberg, J. B., Sutherland, W. M., and Taylor, R. P. (2001) Targeting of *Pseudomonas aeruginosa* in the bloodstream with bispecific monoclonal antibodies. *J. Immunol.* **167,** 2240–2249

32. Lillehoj, E. P., Kim, B. T., and Kim, K. C. (2002) Identification of *Pseudomonas aeruginosa* flagellin as an adhesin for Muc1 mucin. *Am. J. Physiol. Lung Cell. Mol. Physiol.* **282,** L751–L756

33. Lillehoj, E. P., Kim, H., Chun, E. Y., and Kim, K. C. (2004) *Pseudomonas aeruginosa* stimulates phosphorylation of the airway epithelial membrane glycoprotein Muc1 and activates MAP kinase. *Am. J. Physiol. Lung Cell. Mol. Physiol.* **287,** L809–L815

34. Wang, P., Zhang, J., Bian, H., Wu, P., Kuvelkar, R., Kung, T. T., Crawley, Y., Egan, R. W., and Billah, M. M. (2004) Induction of lysosomal and plasma membrane-bound sialidases in human T-cells via T-cell receptor. *Biochem. J.* **380,** 425–433

35. Bonten, E., van der Spoel, A., Fornerod, M., Grosveld, G., and d'Azzo, A. (1996) Characterization of human lysosomal neuraminidase defines the molecular basis of the metabolic storage disorder sialidosis. *Genes Dev.* **10,** 3156–3169

36. Amith, S. R., Jayanth, P., Franchuk, S., Finlay, T., Seyrantepe, V., Beyaert, R., Pshezhetsky, A. V., and Szewczuk, M. R. (2010) Neu1 desialylation of sialyl α-2,3-linked β-galactosyl residues of TOLL-like receptor 4 is essential for receptor activation and cellular signaling. *Cell. Signal.* **22,** 314–324

37. Duca, L., Blanchevoye, C., Cantarelli, B., Ghoneim, C., Dedieu, S., Delacoux, F., Hornebeck, W., Hinek, A., Martiny, L., and Debelle, L. (2007) The elastin receptor complex transduces signals through the catalytic activity of its Neu-1 subunit. *J. Biol. Chem.* **282,** 12484–12491

38. Antonicelli, F., Bellon, G., Lorimier, S., and Hornebeck, W. (2009) Role of the elastin receptor complex (S-Gal/Cath-A/Neu-1) in skin repair and regeneration. *Wound Repair Regen.* **17,** 631–638

39. Jayanth, P., Amith, S. R., Gee, K., and Szewczuk, M. R. (2010) Neu1 sialidase and matrix metalloproteinase-9 cross-talk is essential for neurotrophin activation of Trk receptors and cellular signaling. *Cell. Signal.* **22,** 1193–1205

40. Hinek, A., Bodnaruk, T. D., Bunda, S., Wang, Y., and Liu, K. (2008) Neuraminidase-1, a subunit of the cell surface elastin receptor, desialylates and functionally inactivates adjacent receptors interacting with the mitogenic growth factors PDGF-BB and IGF-2. *Am. J. Pathol.* **173,** 1042–1056

41. Liu, Y. C., Yen, H. Y., Chen, C. Y., Chen, C. H., Cheng, P. F., Juan, Y. H., Chen, C. H., Khoo, K. H., Yu, C. J., Yang, P. C., Hsu, T. L., and Wong, C. H. (2011) Sialylation and fucosylation of epidermal growth factor receptor suppress its dimerization and activation in lung cancer cells. *Proc. Natl. Acad. Sci. U.S.A.* **108,** 11332–11337

42. Kawaguchi, T., Matsumoto, I., and Osawa, T. (1974) Studies on hemagglutinins from *Maackia amurensis* seeds. *J. Biol. Chem.* **249,** 2786–2792

43. Wu, W., Punt, J. A., Granger, L., Sharrow, S. O., and Kearse, K. P. (1997) Developmentally regulated expression of peanut agglutinin (PNA)-specific glycans on murine thymocytes. *Glycobiology* **7,** 349–356

44. Morreau, H., Galjart, N. J., Willemsen, R., Gillemans, N., Zhou, X. Y., and d'Azzo, A. (1992) Human lysosomal protective protein. Glycosylation, intracellular transport, and association with β-galactosidase in the endoplasmic reticulum. *J. Biol. Chem.* **267,** 17949–17956

45. Beguinot, L., Lyall, R. M., Willingham, M. C., and Pastan, I. (1984) Downregulation of the epidermal growth factor receptor in KB cells is due to receptor internalization and subsequent degradation in lysosomes. *Proc. Natl. Acad. Sci. U.S.A.* **81,** 2384–2388

46. Kato, K., Lillehoj, E. P., Kai, H., and Kim, K. C. (2010) MUC1 expression by human airway epithelial cells mediates *Pseudomonas aeruginosa* adhesion. *Front. Biosci.* **2,** 68–77

47. Liang, F., Seyrantepe, V., Landry, K., Ahmad, R., Ahmad, A., Stamatos, N. M., and Pshezhetsky, A. V. (2006) Monocyte differentiation up-regulates the expression of the lysosomal sialidase, Neu1, and triggers its targeting to the plasma membrane via major histocompatibility complex class II-positive compartments. *J. Biol. Chem.* **281,** 27526–27538

48. Lukong, K. E., Seyrantepe, V., Landry, K., Trudel, S., Ahmad, A., Gahl, W. A., Lefrancois, S., Morales, C. R., and Pshezhetsky, A. V. (2001) Intracellular distribution of lysosomal sialidase is controlled by the internalization signal in its cytoplasmic tail. *J. Biol. Chem.* **276,** 46172–46181

49. Nan, X., Carubelli, I., and Stamatos, N. M. (2007) Sialidase expression in activated human T lymphocytes influences production of IFN-γ. *J. Leukoc. Biol.* **81,** 284–296

50. Hanisch, F. G., Stadie, T., and Bosslet, K. (1995) Monoclonal antibody BW835 defines a site-specific Thomsen-Friedenreich disaccharide linked to threonine within the VTSA motif of MUC1 tandem repeats. *Cancer Res.* **55,** 4036–4040

51. Uehara, F., and Ohba, N. (2002) MUC1 and sialoglycan expression associated with cytotoxic T lymphocyte infiltration in eyelid malignant tumors. *Jpn. J. Ophthalmol.* **46,** 237–243

52. Meuillet, E. J., Kroes, R., Yamamoto, H., Warner, T. G., Ferrari, J., Mania-Farnell, B., George, D., Rebbaa, A., Moskal, J. R., and Bremer, E. G. (1999) Sialidase gene transfection enhances epidermal growth factor receptor activity in an epidermoid carcinoma cell line, A431. *Cancer Res.* **59,** 234–240

53. Monti, E., Bassi, M. T., Papini, N., Riboni, M., Manzoni, M., Venerando, B., Croci, G., Preti, A., Ballabio, A., Tettamanti, G., and Borsani, G. (2000) Identification and expression of NEU3, a novel human sialidase associated to the plasma membrane. *Biochem. J.* **349,** 343–351

54. Yamaguchi, K., Hata, K., Wada, T., Moriya, S., and Miyagi, T. (2006) Epidermal growth factor-induced mobilization of a ganglioside-specific sialidase (NEU3) to membrane ruffles. *Biochem. Biophys. Res. Commun.* **346,** 484–490

55. Beachey, E. H. (1981) Bacterial adherence: adhesin-receptor interactions mediating the attachment of bacteria to mucosal surface. *J. Infect. Dis.* **143,** 325–345

56. Saiman, L., and Prince, A. (1993) *Pseudomonas aeruginosa* pili bind to asialoGM1 which is increased on the surface of cystic fibrosis epithelial cells. *J. Clin. Investig.* **92,** 1875–1880

57. Gupta, S. K., Masinick, S., Garrett, M., and Hazlett, L. D. (1997) *Pseudomonas aeruginosa* lipopolysaccharide binds galectin-3 and other human corneal epithelial proteins. *Infect. Immun.* **65,** 2747–2753

58. Schroeder, T. H., Lee, M. M., Yacono, P. W., Cannon, C. L., Gerçeker, A. A., Golan, D. E., and Pier, G. B. (2002) CFTR is a pattern recognition molecule that extracts *Pseudomonas aeruginosa* LPS from the outer membrane into epithelial cells and activates NF-κB translocation. *Proc. Natl. Acad. Sci. U.S.A.* **99,** 6907–6912

59. Zhang, J., Xu, K., Ambati, B., and Yu, F. S. (2003) Toll-like receptor 5-mediated corneal epithelial inflammatory responses to *Pseudomonas aeruginosa* flagellin. *Invest. Ophthalmol. Vis. Sci.* **44,** 4247–4254

60. Soong, G., Reddy, B., Sokol, S., Adamo, R., and Prince, A. (2004) TLR2 is mobilized into an apical lipid raft receptor complex to signal infection in airway epithelial cells. *J. Clin. Investig.* **113,** 1482–1489

61. Pastoriza Gallego, M., and Hulen, C. (2006) Influence of sialic acid and bacterial sialidase on differential adhesion of *Pseudomonas aeruginosa* to epithelial cells. *Colloids Surf. B Biointerfaces* **52,** 154–156

62. McAuley, J. L., Linden, S. K., Png, C. W., King, R. M., Pennington, H. L., Gendler, S. J., Florin, T. H., Hill, G. R., Korolik, V., and McGuckin, M. A. (2007) MUC1 cell surface mucin is a critical element of the mucosal barrier

rier to infection. *J. Clin. Investig.* **117,** 2313–2324

63. Costa, N. R., Mendes, N., Marcos, N. T., Reis, C. A., Caffrey, T., Hollingsworth, M. A., and Santos-Silva, F. (2008) Relevance of MUC1 mucin variable number of tandem repeats polymorphism in *H. pylori* adhesion to gastric epithelial cells. *World J. Gastroenterol.* **14,** 1411–1414

64. Parker, P., Sando, L., Pearson, R., Kongsuwan, K., Tellam, R. L., and Smith, S. (2010) Bovine Muc1 inhibits binding of enteric bacteria to Caco-2 cells. *Glycoconj. J.* **27,** 89–97

65. Varki, A. (1997) Sialic acids as ligands in recognition phenomena. *FASEB J.* **11,** 248–255

66. Bremer, E. G., Schlessinger, J., and Hakomori, S. (1986) Ganglioside-mediated modulation of cell growth. Specific effects of GM3 on tyrosine phosphorylation of the epidermal growth factor receptor. *J. Biol. Chem.* **261,** 2434–2440

67. Li, Y., Ren, J., Yu, W., Li, Q., Kuwahara, H., Yin, L., Carraway, K. L, 3rd, and Kufe, D. (2001) The epidermal growth factor receptor regulates interaction of the human DF3/MUC1 carcinoma antigen with c-Src and β-catenin. *J. Biol. Chem.* **276,** 35239–35242

68. Pochampalli, M. R., el Bejjani, R. M., and Schroeder, J. A. (2007) MUC1 is a novel regulator of ErbB1 receptor trafficking. *Oncogene* **26,** 1693–1701

69. Amith, S. R., Jayanth, P., Franchuk, S., Siddiqui, S., Seyrantepe, V., Gee, K., Basta, S., Beyaert, R., Pshezhetsky, A. V., and Szewczuk, M. R. (2009) Dependence of pathogen molecule-induced toll-like receptor activation and cell function on Neu1 sialidase. *Glycoconj. J.* **26,** 1197–1212

70. d'Azzo, A., and Bonten, E. (2010) Molecular mechanisms of pathogenesis in a glycosphingolipid and a glycoprotein storage disease. *Biochem. Soc. Trans.* **38,** 1453–1457

71. Buccoliero, R., Palmeri, S., Ciarleglio, G., Collodoro, A., De Santi, M. M., and Federico, A. (2007) Increased lung surfactant phosphatidylcholine in patients affected by lysosomal storage diseases. *J. Inherit. Metab. Dis.* **30,** 983

72. Starcher, B., d'Azzo, A., Keller, P. W., Rao, G. K., Nadarajah, D., and Hinek, A. (2008) Neuraminidase-1 is required for the normal assembly of elastic fibers. *Am. J. Physiol. Lung Cell. Mol. Physiol.* **295,** L637–L647

73. Champigny, M. J., Johnson M., and Igdoura, S. A. (2003) Characterization of the mouse lysosomal sialidase promoter. *Gene* **319,** 177–187

74. Olayioye, M. A., Neve, R. M., Lane, H. A., and Hynes, N. E. (2000) The ErbB signaling network: receptor heterodimerization in development and cancer. *EMBO J.* **19,** 3159–3167

75. Kato, T., Wang, Y., Yamaguchi, K., Milner, C. M., Shineha, R., Satomi, S., and Miyagi, T. (2001) Overexpression of lysosomal-type sialidase leads to suppression of metastasis associated with reversion of malignant phenotype in murine B16 melanoma cells. *Int. J. Cancer* **92,** 797–804

76. Uemura, T., Shiozaki, K., Yamaguchi, K., Miyazaki, S., Satomi, S., Kato, K., Sakuraba, H., and Miyagi, T. (2009) Contribution of sialidase NEU1 to suppression of metastasis of human colon cancer cells through desialylation of integrin β4. *Oncogene* **28,** 1218–1229

77. Ram, S., Sharma, A. K., Simpson, S. D., Gulati, S., McQuillen, D. P., Pangburn, M. K., and Rice, P. A. (1998) A novel sialic acid binding site on factor H mediates serum resistance of sialylated *Neisseria gonorrhoeae. J. Exp. Med.* **187,** 743–752

78. Anthony, R. M., and Ravetch, J. V. (2010) A novel role for the IgG Fc glycan: the anti-inflammatory activity of sialylated IgG Fcs. *J. Clin. Immunol.* **30,** S9-S14

79. Yoshimura, M., Ihara, Y., Matsuzawa, Y., and Taniguchi, N. (1996) Aberrant glycosylation of E-cadherin enhances cell-cell binding to suppress metastasis. *J. Biol. Chem.* **271,** 13811–13815

80. Steelant, W. F., Recchi, M. A., Noë, V. T., Boilly-Marer, Y., Bruyneel, E. A., Verbert, A., Mareel, M. M., and Delannoy, P. (1999) Sialylation of E-cadherin does not change the spontaneous or ET-18-OMe-mediated aggregation of MCF-7 human breast cancer cells. *Clin. Exp. Metastasis* **17,** 245–253